Development of a Prosthetic Biofeedback Method and Device to Measure Quality of Fit for Trans-Tibial Amputees

by

Robin Murdock

A thesis
presented to the University of Waterloo
in fulfillment of the
thesis requirement for the degree of
Masters of Applied Science of Engineering
in
Mechanical and Mechatronics

Waterloo, Ontario, Canada, 2021

Author's Declaration

I hereby declare that I am the sole author of this thesis. This is a true copy of the thesis, including any required final revisions, as accepted by my examiners.

I understand that my thesis may be made electronically available to the public.

Abstract

As the primary interface between the prosthetic and the residual limb, the socket is a crucial component affecting fit and function of the device. While prostheses have been used for centuries, prosthetic socket design concepts have remained stagnant. With the increase in prevalence of obesity and diabetes, amputations associated with secondary complications have risen as a consequence. In particular, neuropathy complicates transition of a new amputee to using a prosthetic socket crucial for their quality of life by reducing -or in some cases completely hindering- tactile sensation and healing in the residual limb. The objectives of this thesis are to: 1) create a protocol to evaluate innovative technology within the socket in vitro while maintaining a true sense of the users limb geometry and material characteristics that interface with the socket, and 2) develop and validate a method of providing biofeedback to prosthesis users, particularly those with neuropathy.The focus of this thesis will be on trans-tibial amputees and prosthesis to reduce the complexity of including a knee joint and to address the largest population of amputees.

In this thesis, a method of testing innovations through the use of artificial biofidelic limbs by systematically varying dimensions was first developed and validated against in vivo measurement of amputees reported by Silver-Thorn [15]. Materials characterization yielded closely matching relaxation at 5s to published values [15]- achieving a range of 22.43-31.94% to that of Silver-Thorn with a range of 25.35-49.25%. However, full relaxation and size control during fabrication needs improvement to create a more consistent limb. The max relaxation being measured as 39.06% against the in vivo measurements reaching 68.03%. Additionally the size of the limbs varied from the model by a maximum of 13mm.

Following development of the test methods, a method of measuring fit changes within the socket using a single pneumatic (PicoPress) sensor on the distal end to measure distal end (or end-pad) contact pressures. Tests using the biofidelic limbs indicates the use of a single picopress sensor in the distal end is a viable option to detect fit changes over time. However, settling times need to be further investigated to identify barriers to dynamic use (e.g. gait during walking). Feedback from practicing orthotists indicate the PicoPress approach is a viable option to include in existing fabrication processes used to generate custom sockets without altering supply lead times and fabrication times.

Acknowledgements

I would like to thank all the people who made this thesis possible. Particularly James Tung for his immense patience and unmatched guidance both outside and inside the lab while working on my thesis. I also want to thank the Neural and Rehabilitation Engineering Lab for their help and laughs throughout my thesis as well as my colleagues at the University of Waterloo.

I want to extend a special thank you to those who helped me with my thesis, in particular the Undergraduate Research Assistants (URAs), Andrew Laing, Stewart McLachlin, and especially Prosthetic Ability and Doug Dittmer for their guidance and expertise in making this thesis possible.

Table of Contents

List of Figures

1 Introduction

The leading cause of lower limb amputations in North America is complications arising from diabetes or cardiovascular related health conditions [5]. Considering the increase in prevalence of obesity and diabetes, amputations associated with secondary complications have risen as a consequence. Typical lower limb amputees receive their first prosthetic within the first two weeks of their amputation as their first transition into the daily challenges that they may have to face and overcome. Providing a prosthetic that has ease of use and functionality to facilitate independent mobility and quality of life is crucial to a users' transition.

As the primary interface between the prosthetic and the residual limb, the socket is a crucial component to the device. While prostheses have been used for centuries, a redesign of the prosthetic socket has not undergone significant innovation since its initial creation in the 16th century with the exception of material advances, transitioning from using wood and metals to user much lighter weight, durable and easier to form thermoplastics. However, in terms of the actual function, there is little differences to those designs compared to current socket designs. Many of the designs since the first prosthetic rely on an interface which would translate the individuals weight into a rod and then a peg or foot. This general concept is still used today with a new way to transfer that weight only recently introduced for trans tibial amputees in the 1950s with the introduction of the PTB socket.

While custom-fabricated sockets molded to users' residual limbs (via a plaster mould method) continue to be the standard approach for socket design for most lower limb amputees, there exist many well-known problems. An unaddressed issue in the prosthesis field is the high level of reports of discomfort or improper fit in clinics [6], marking an area for improvement. This problem is greater when one considers individuals with diabetes or cardiovascular disease who experience peripheral neuropathy. Peripheral neuropathy occurs when the nerves that carry messages to and from the brain and spinal cord are damaged, a common complication of poor blood circulation resulting in damage to the nerves in the limb. When it comes to a prosthetic, this becomes problematic as it leaves users of lower limb prosthesis the inability to gain feedback regarding their socket interface fit from mechanoreceptors, sensory receptors that send information via the nervous system and providing information to the brain like pain.

By the time the improper fit is recognized by the user, tissue damage has often been done. Poor socket fit also impacts functional characteristics, such as gait, which can lead to a variety of problems including (but not limited to)

pressure sores and hip problems. Comfort and fit is exacerbated by the fact that the residual limb itself is a dynamic system. In particular, lower limb volume fluctuations caused by swelling, sweating, injury, salt levels, and more, can change limb volume an average of +/- 10% a day [7]. These volume fluctuations change the interface of the socket, which can result in pressure being transferred to "pressure sensitive" areas of the residual limb. More sensitive to pain and vulnerable to pressure sores, pressure sensitive areas typically avoid load-bearing pressures (Fig 1).

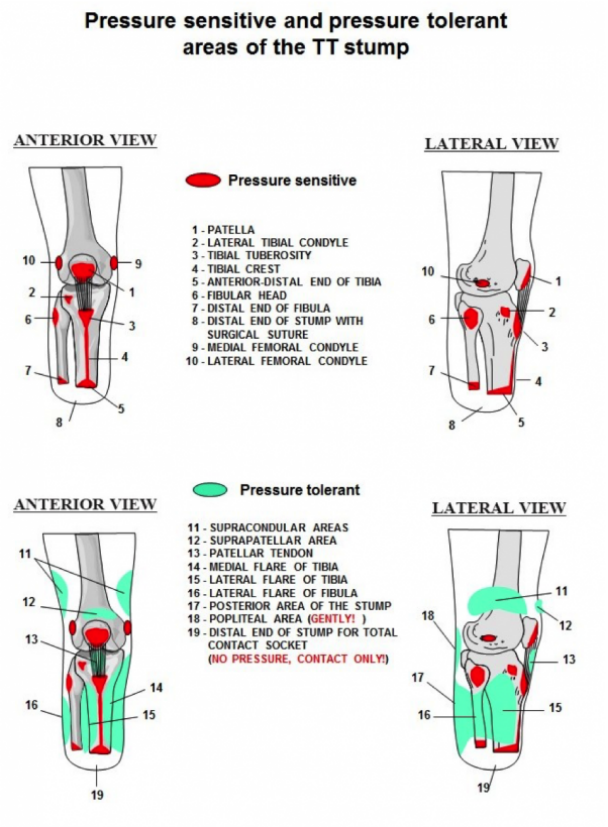

Figure 1: Trans Tibial Tolerant and Sensitive Pressure Zones[1]

While there has been a surge in innovation for prosthetic manipulanda (or end-effectors), current socket interface design rooted in traditional approaches suggests a significant change is needed. The goal of this thesis was to develop a device to sense socket fit changes associated with volume changes and a system to test such devices was also investigated.

The specific objectives of this thesis were to: (1) create in vitro methodologies to systematically test new socket technologies addressing fit that simulates

the surface geometry and volume changes of a true limb (2) create and test a sensor to provide socket fit feedback to users. Chapter 2 will cover the history, current relevant technology, and the limitations of these technologies. Chapter 3 will describe a methodology for custom socket ft testing and validation through the development of biofidelic limbs. Chapter 4 will describe a socket sensing prototype and chapters 5 and 6 will discuss and conclude the thesis work.

The advances described in this thesis will permit a greater understanding of the socket-limb interface dynamics under everyday conditions, including while moving. The novel biofidelic limb method can be used to assess current systems designed to resolve volume change and fit issues, including the effectiveness of alternate prosthetic socket designs.

2 Background

2.1 Historical perspective

Amputation dates back as far as 5000 B.C. and the first prosthetic limb was seen 16th century with a mostly metal composition and a socket to limb interface similar to what we see today [2] .

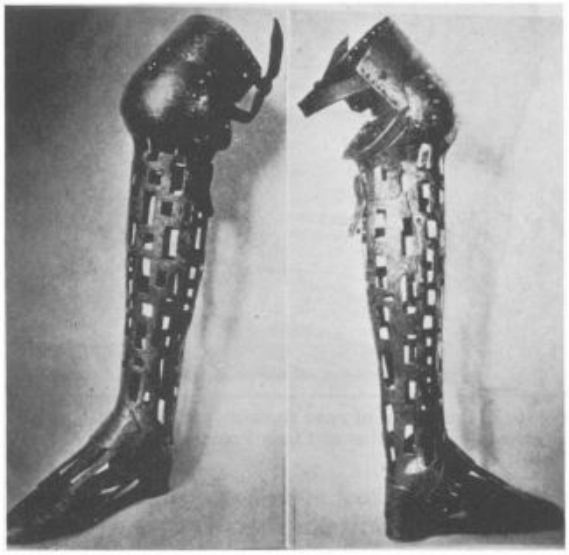

Figure 2: 16th Century Prosthetic [2]

The limb from Figure 4 shows the 16th century limb including perforations to reduce weight, indicating the challenges of available materials to innovate and improve quality of life of amputees. Throughout the years, the general concepts of prosthetics design have remained the same. Simply reducing weight and appearance by changing the material, such as transitioning from metal to wood [2].

In the modern world, we have changed much in the way of prosthetics functionality through specialized design, such as lower-limb 'blade' designs optimized for runners. Modern innovations have been highlighted by advances in the control and functionality of prostheses with the goal of improving the quality of life and returning or even improving the functionality of the limb. These innovations include powered/actuated limbs, targeted muscular re-innervation technology to return the control to the users' nervous system, automatic knee and elbow joint mechanisms, and haptic (and proprioception) feedback.

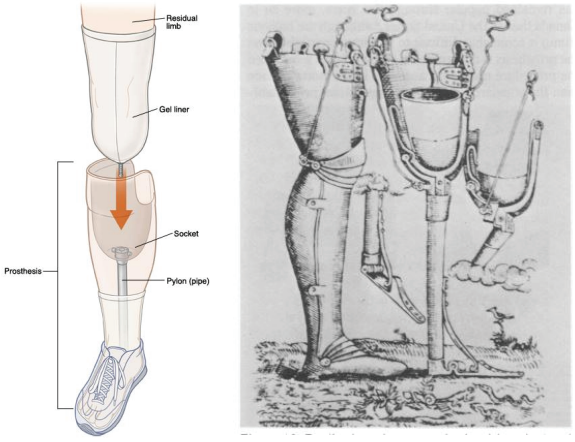

Figure 3: Socket Comparison- Modern Left; 16th Century Right[2]

2.2 Socket design

A critical issue with many of the aforementioned advances is the relative lack of innovation in socket interface design. Published socket innovations add weight to the prosthetic (e.g., actuators, batteries), exacerbating poor interfacing between the user and prosthetic, evidenced by reported complaints by myoelectric and robotic prosthetic users [8]. Without improving the socket, the goals of improving quality of life and functionality remain limited since it is the primary mechanical interface between the user and the device. Ultimately, the socket design is a critical factor in accepting or rejecting the prosthetic.

Generally, the interface mechanism(s) have not changed significantly since the 16th century. On the left panel in Figure 3, a modern socket is shown with a gel liner and socket as the interface along with the limb and sock layer. The 16th century sockets use the same mechanism to bear weight, comprising of a socket, liner, and (in some cases) an end-pad. While socket innovation has stagnated there has been advances to the manufacturing and materials methods like the introduction of thermoplastics, polyurethane foams, gel liners, and molding techniques to fabricate fully customized and light weight sockets.

The most recent and significant developments in socket applications have been the advent of the Patellar Tendon Bearing (PTB) socket in the 1950s [7]. The PTB socket is the most common socket design in use today, with good versatility particularly within the first 12-18 months after amputation when the residual limb fluid fluctuations, inflammation, and skin sensitivities are highest. A PTB socket design, as shown in Figure 4, is compromised of several parts: socket, liner, pylon, prism connector and prosthetic foot. The user places a sock over their limb and then places it inside the socket. The liner creates an additional shock absorption layer between the user and the interface.

Alternative to prosthetic sockets include invasive surgical techniques such as osseointegration. Osseointegration is a surgical technique wherein the load bearing aspect of a socket is integrated into the existing bone of the patient. This is done by drilling a hole into the bone and implanting a rod, which is integrated into the skeletal system as bone grows around the rod. While osseointegration continues to gain attention and momentum, several limitations challenge widespread adoption which will be discussed in the next section.

Figure 4: PTB socket diagram [3]

This thesis is focused on the process of rectification, where the socket is custom built to the user's limb geometry using a method that involves taking a negative and positive mold which is then adjusted by hand to improve fit. In general, socket designs aim to redistribute pressures away from intolerant areas and to tolerant areas of the limb, as shown in Figure 1. At pressure-intolerant areas, pressure is relieved by creating more space (i.e., removing material) such as directly interfacing with bony prominences. By building up material interfacing with tissues tolerant to pressure, prosthetists aim to redistribute loads away from sensitive areas. The pylon transfers the weight of the user from the socket interface into the foot and the ground. The foot creates support around the ankle joint, controls ground reaction forces, and absorbs shocks. This setup will typically include an end pad, typically flexible foam, which acts as a cushioning on the distal end of the residual limb.

2.3 Limitations of current socket systems

The key issue with current socket designs are the physiological changes in the amputees' limb that cause fluctuations in residual limb volume. Volume changes are affected by many factors, including hydration, inflammation, diet, and/or circulation. Decreased limb volume can cause the limb to 'sink' inside the socket, leading to poor pressure distribution over the socket interface. As a key 'pressure-intolerant' area, increased pressures on the distal end of the limb (i.e., surgical area) can cause abrasion on the sutures, scars, and undue pressure(s) on the cut bone. Furthermore, common co-morbidities associated with amputee characteristics amplify the risk of secondary complications.

2.3.1 Pressure ulcers

Pressure ulcers (or ulcers) are wounds arising from long exposure to high pressures, leading to necrosis and tissue damage. If not treated, this tissue damage can become infected and ultimately gangrenous. This can be especially problematic for amputees[9] who have a predisposition of vascular disease. This can cause limited to no sensation in the lower limb, making it difficult for users to recognize ulcers, cuts or other pain. This leads to ulcers going unnoticed, often leading to higher risk of gangrenous ulcers, and can ultimately lead to the rejection of the prosthetic. A common cause for rejection of the prosthetic is frequent ulcers requiring significant time without the device to permit healing. Without proper healing, the ulcer can ultimately lead to further amputation or surgery.

2.3.2 Co-morbidities

Considering that 54/text% of transtibial amputations in North America are due to vascular complications including diabetes [10], characteristics of this population must be considered. In particular, the effect of diabetes on tactile sensation and slow healing both contribute to an increased risk of pressure ulcers.

Diabetic amputees face two issues related to socket fit: 1) peripheral neuropathy, specifically the loss of tactile sensation in the limbs, and 2) poor vasculature and circulation in the periphery, increasing the risk of infection and reducing healing rates. Ideally, a prosthetic user regularly checks and maintains their lower limb with regular skin inspections in order to identify any redness or skin breakdown, adjust fit (if necessary), and reporting to their physician or orthotist. The reality is that most amputees receive insufficient education of socket design fit management and/or are challenged to consistently manage lower limb skin integrity, leading to significant problems that go unnoticed or unaddressed. Not only are skin breakdowns associated with socket fit, but proper function is highly dependent on interface integrity. In particular, poor socket fit can lead to gait compensation introducing risk of secondary complications (e.g., hip issues). This can cause pain and the need to discontinue use of the device, which ultimately limits the users quality of life.

2.4 Socket design approaches

Current solutions to address volume changes in the residual limb and maintain a well-fitting prosthetic interface are conducted through the use of liners, socks, pads, adjustable sockets and vacuum actuated sockets [8]. Liners, including gel and hydrostatic versions, aim to address volume changes by dampening movement effects (i.e., pistoning). Actuated sockets address the issue by changing the size of the socket through pump mechanisms and user input via handheld controller, avoiding the need to remove the socket. A key issue with the actuated socket systems is the need for additional pump and control system components, adding cost and weight to the device. Furthermore, a limiting factors of the aforementioned solutions is the need for user-initiated adjustments. Users are required to intervene and adjusting to the appropriate fit, confounded by the lack of pressure and/or pain sensation associated with neuropathy. Many users may lack the sensory capabilities required to adjust socket fit appropriately. Furthermore, most amputees may not receive (or retain) education on self-managed residual limb health and maintenance [11].

As a means to permit load-bearing through the bone, osseointegration has proven to be viable for those who qualify. While osseointegration appears to be a viable alternative to current PTB socket design, the procedure is more invasive. Specifically, amputees with cardiovascular diseases (e.g., diabetes) or conditions affecting bone density or quality (e.g., osteoporosis) are less suitable (and often contraindicated) for osseointegration. As an invasive surgery, osseointegration procedures are associated with long healing times (with no weight bearing) and rigorous skin maintenance near the integration contact.

2.5 Knowledge and methodological gaps

Thus, a method of educating/guiding users on residual limb maintenance as well as a method to provide biofeedback on interface fit is needed. With proper guidance and feedback, the liners and socks currently used to regulate prosthetic fit will be more effective while maintaining a low cost.

Biofeedback has been studied in many facets and shown to be useful for any learnable response impeded by poor perception, such as neuropathy [12]. Proper feedback visualization and presentation is needed in order to motivate and create a proper knowledge transfer to the user. Auditory/visual and tactile feedback all contribute to a better somatosensory feedback system [13]. While tactile feedback is a viable approach, their application to the proposed biofeedback sensor is beyond the scope of the current thesis.

2.6 Regulatory requirements

Prosthetic sockets fall under a Class 1 medical device standard for both FDA and Health Canada regulatory bodies. As a Class 1 device, prosthetic socket manufacturers are mandated to follow general quality control guidelines and to

be registered with ISO 19485. General controls requires extensive documentation including registrations of producers of the product, reports of repairs, replacements, refunds, recalls, event reports, and device tracking for devices intended for human use ("520" of FDC Act which includes exemptions and manufacturing practice requirements)[14]. For Class 1 devices that fall under the category of prostheses, additional documentation of risk/benefits are not required (unless requested due to complaints or adverse events).

In comparison, Class 2 devices require more stringent documentation including performance standards, post market surveillance, patient registries. Prior to wide distribution, pre-market data requirements for Class 2 device certification includes performance and risk metrics creating market barriers limiting innovation. As sockets advance with actuated components and osseointegrated into internal tissues, regulatory bodies will require new means of validating risk, evaluating benefits, and measuring performance.

Biofidelic limbs have been used to evaluate effectiveness of a variety of products, such as orthotic braces, helmets, and hip protectors. A series of systematically varying biofidelic limbs could aid in documenting socket innovations by providing the ability to test performance metrics before needing human trials, reducing the cost and risk to both the companies and users. Biofidelic limbs may also provide a means to better understand the impact of residual volume changes on interface pressures within the prosthetic. Our current understanding of interface integrity relies on in vivo studies with low sample sizes, limiting generalizability for guiding development.

3 Biofidelic Limbs and Standardized Socket Testing Methods

3.1 Introduction

Socket design and fabrication is a critical factor in the utility and satisfaction of prosthetic devices, requiring significant time and financial cost to customize, evaluate, and maintain. In Ontario (Canada), the cost of prosthetic fitting is covered by public health insurance up to 75% for the initial fitting and purchase of the first prosthetic. Further costs, such as frequent socket modifications, are not or partially covered. Hence, it is less costly for users if their initial fitting is done well and no skin health issues arise. For prosthetists, improving socket design methods would translate to fewer follow-up appointments and better outcomes for their clients.

The prosthetic field lacks efficient methods and tools to assess socket fit, largely due to heterogeneity in residual limb geometry requiring custom socket designs. While human trials are the ideal approach to testing of new socket systems, they are a costly endeavor as a primary testing method for new products. For stakeholders including users, doctors, prosthetists, component manufacturers, standardized testing and validation methodologies for new socket methods and products would facilitate innovation (e.g., new methods for designing, evaluating sockets). For users who participate in trials, it can be frustrating to be constantly used as the method of validating products that may never move to market. Computational simulation approaches (e.g., finite element modelling) can potentially predict socket design effects, but remain rudimentary and without efficient pipelines to account for individual variation in residual limb geometry like seen in Pathak, 1998; Zhang, 1996 and more[15][16][17][18]. These methodological limitations are becoming increasingly problematic for inventors of emerging socket technologies, slowing progress by having in-sufficient testing before moving to user trials which can be costly and slow especially if the product is not well received.

Current testing methods outside of human trials include computational methods (e.g., simulations) and simplified test protocols (e.g., balloons). Simulation software are challenged by the time required to generate meaningful outputs, including acquiring custom geometry and tissue properties, as well as difficulty translating model estimates to real-world values. Simulation-based analysis may be useful for large companies with available resources for the personnel, testing machines and time to tackle what is need to produce an appropriate model. Balloon testing methods, using a partially-filled latex balloon, are limited in considering the interaction of limb properties (e.g. geometry and material characteristics). Socket comfort, fit, and standardized testing are important factors in improving prosthetic use and increasing the quality of life of amputees and thus a better method to test these properties is needed. Creating a biofidelic limb that can replicate the geometry and the volume changes is needed; par-

ticularly in the ranges of +/- 10% which is the average change that amputees experience throughout a day [7].

Currently 49% of amputees stopped using their prosthesis due to self-reported comfort issues, and 51% reported the prosthesis offered them no additional function [6]. When users report discomfort, this is typically referring to improper fit linked to changes in pressure distribution to sensitive and/or pressure intolerant areas. In many circumstances, prosthetic function is influenced by socket fit issues causing the amputee to slow down (e.g., reduced walking speed, poorer balance, withdrawal from activity) and/or impair the full function of their prosthesis [11]. Quality of life, contribution to society, and motivation can all be affected at the transitional stage post amputation to their initial (temporary) socket. Fit parameters, which are reflective of comfort, can be quantified reliably by analyzing the pressure interface from human to socket. Considering socket innovation has stagnated since the Patella Tendon Bearing (PTB) socket developed in 1950s [19], advancing systematic testing targeted at objective parameters (i.e., fit, function) will remove barriers to socket innovation.

Evolving regulatory requirements may provide the impetus to advance socket testing methods. Currently, prosthetic sockets fall under a class 1 medical device standard for both FDA and Health Canada regulatory bodies. As a class 1 device, prosthetic socket manufacturers are only required to follow general quality control guidelines (ISO 19485 registration). For class 1 devices that fall under the category of prostheses, documentation of additional risk/benefits are not required unless requested due to complaints or reported adverse events. Considering standard metrics of proper fit and function are lacking in this field, and not required for device certification, there is little incentive for the quality and testing of prosthetic devices for functioning. Innovations in powered and myoelectric prostheses will be classified as class 2 devices, requiring more stringent device testing. Thus, new methods to test socket concepts and functionality are needed for the prosthetic industry to bring these advances to market.

In this thesis, we are motivated to advance testing methods to quantify fit across a range of conditions simulating a common problem: volume change. This chapter aims to develop a method of fabricating biofidelic limbs capable of meeting geometric shape and material properties of residual limbs. The fabricated limbs were tested using a rate-controlled indentor to measure the material characteristics compared to data reported by Silver-Thorn, 1999 [4].

3.2 Methods

This section first describes methods employed to fabricate the biofidelic limbs, followed by procedures used for materials testing.

3.2.1 Outer Layer

In conjunction with certified orthotists at Prosthetic Ability, a mold of an amputee's residual limb was created using a Hands On wrap cast method with

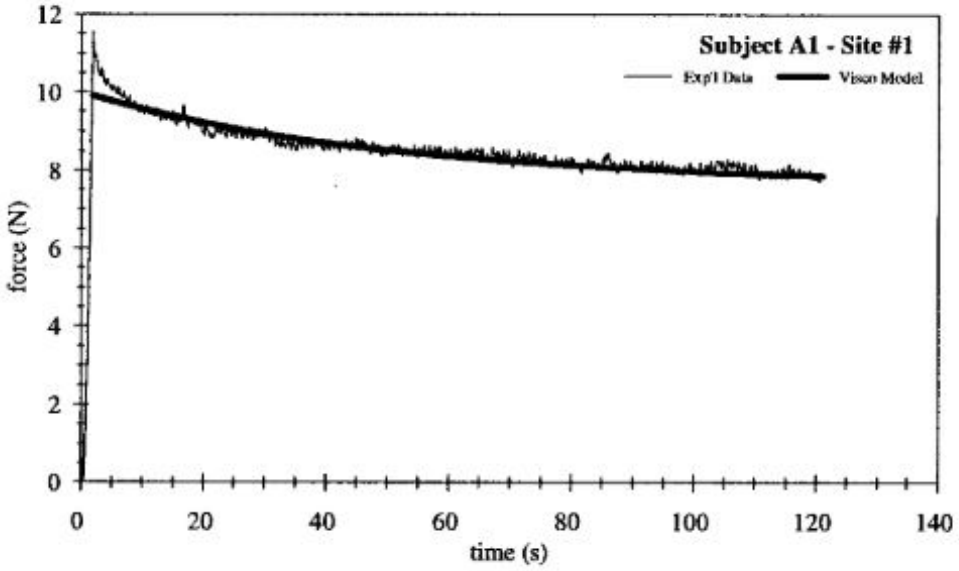

Figure 5: Relaxation Data of an Amputee limb at popliteal location [4]

plaster of paris (POP)[2]. This mold was 3D scanned with AICON SmartScan (Hexagon Manufacturing Intelligence, Cobham, UK) optical scanner with the assistance of the Multi-scale Additive Manufacturing Laboratory (MSAM). The scanned model was imported to Meshmixer (Autodesk Research, San Rafael, CA, USA) to resolve holes using the hole detection function. Smoothing to remove artifacts associated with the porous surface of the plaster was manually conducted using the surface "robust smoothing" tool (strength: 50, size: 30). The excess upper (proximal) part of the limb (i.e., not used in socket design) was manually cut out of the mesh, as it is not part of the limb. The limb was then duplicated internally and fused to create a 6.5mm thick shell, the minimum allowable for 3D printing, without altering the external size and shape as seen in Figure 6.

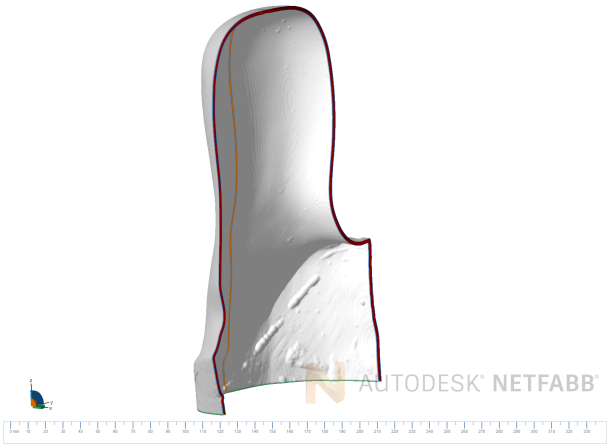

Figure 6: Limb Shell Cross Section

This shell was saved for use as the outer layer of the proposed biofidelic limb. The limb was scaled by +/- 10% in the x and y (radial) directions to create two limb models of sizes reflecting reported daily volume fluctuations in transtibial amputees. Initially, exported limb meshes (via STL) demonstrated mesh resolutions too poor for slicing using Netfabb (Netfabb, Autodesk Inc. Mill Valley California, USA). After refining the mesh level detail by a factor of 3 in the Meshmixer software, the mesh resulted in a smooth geometry, as shown in Figure 7.

Figure 7: Limb Shell Mesh Curved Ridge

Additionally, the lower portion of the limb created a ridge-like transition not part of the original limb (see Figure 6), due to the extra material created by the container used to generate the initial plaster mold. The section defined by the ridge was removed and smoothed to create a more accurate limb profile

that will interact with the socket in a more expected manner, since the ridge was removing the pressure applied acting as a "cap" and limiting the limb from moving further into the socket, this improvement can be seen in Figure 8.

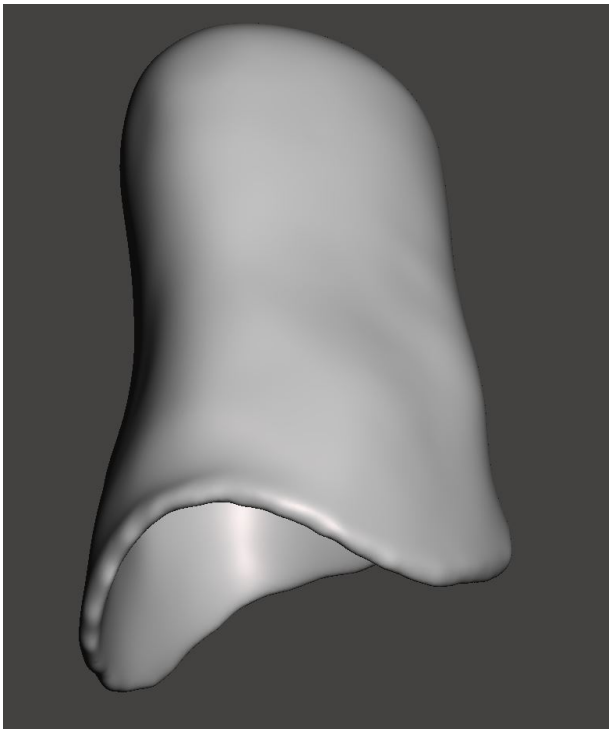

Figure 8: Final Limb Shell +10. Image is zoomed in to visualize the mesh resolution along the edge used to trim excess surface material.%

The limbs were then printed with a Stratasys J750 (Stratasys, Ltd., Eden Prairie, Minnesota, United States) using their polymer based material called Tango Plus with a shore value (a hardness value which measures the resistance to a spring loaded indentor) of 30, converted from reported tissue values of 34.4 - 14.1 kN/m. [20]. The final result of a limb outer shell before the ridge was removed can be seen in Figure 9 below:

3.2.2 Inner section

In this section, the fabrication processes to generate the inner layers simulating soft tissues and the tibia are described. The flexible (skin) outer layer was suspended in a hole cut into a plywood sheet fixed to a workbench. An acrylic sheet cut in half with semi-circular cutouts was gently fixed to the top of the

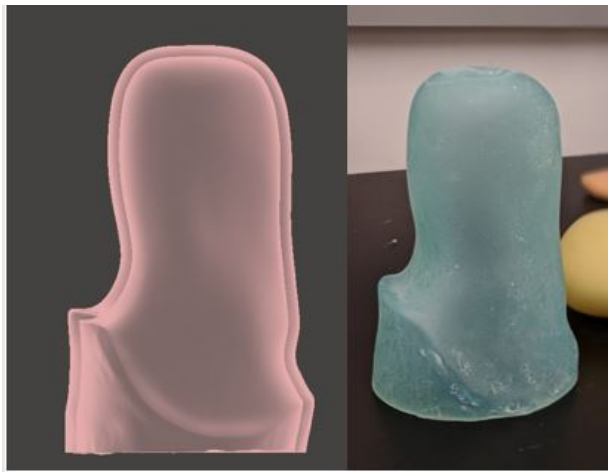

Figure 9: Outer Shell Final Product

socket to hold the outer layer into place and reduce the width of the hole for expanding foam material to be applied.

Flexfoam V! (Flexfoam V!, Flexfoam, Phoenix Arizona, USA) hardening and base agents were mixed (in a plastic cup) with a 50/50 ratio, and mixed vigorously for 60s or until warm on the hands through the cup. The mix was poured in the outer (skin) layer and plastic wrap was taped across the top to enclose the foam. To simulate the tibia, an aluminun rod (Wall thickness=1.651mm OD=19.05mm) was selected to approximate material characteristics of published values on bone properties. While the foam was curing the aluminum rod was placed perpendicular to the bottom of the limb and held in place using a vice clamp approximately 25.4 mm from the distal end inner surface. A level was used to confirm the rod angle prior to curing. After curing, the plastic wrap was removed and the limb was inspected under a light to ensure no bubbles and/or cavitations occurred during the curing process. Inspections were conducted by shining a light through the foam and searching for shadows in the bubbles, allowing easy detection through the translucent mold.

These steps lead to the final result as seen below as a fully completed biofidelic limb.

3.2.3 Mechanical Testing

Following generation of prototype biofidelic limbs, mechanical properties were tested in comparison to *in vivo* tissue characteristics. In particular, Silver-Thorn reported *in vivo* skin indentation test results in a sample of amputees [4]. In order to test the prototype, a Cellscale: Univert Universal Testing Machine (UTM) was used (Univert, Cellscale Biomaterials Testing, Waterloo, Ontario, CA). Developed to match the methodology used by Silver-Thorn, the rate-

Figure 10: Final Limb Product

controlled indentation tests were conducted using a 4mm diameter indentor with 10mm length in 3 critical locations: patellar, popliteal and fibular head locations. Once a 1 N force was achieved by the UTM, the test began by advancing the indentor with a 10 mm/s speed up to 10 mm deflection then retracted in a single cycle. Ten (10) cycles were conducted for each location on one full-scale limb and one 10% larger (circumferentially).

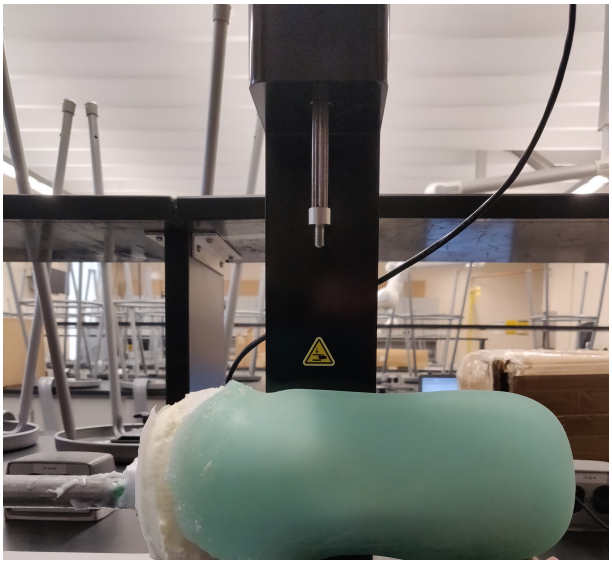

Figure 11: Placement of biofidelic limbs underneath the indenter

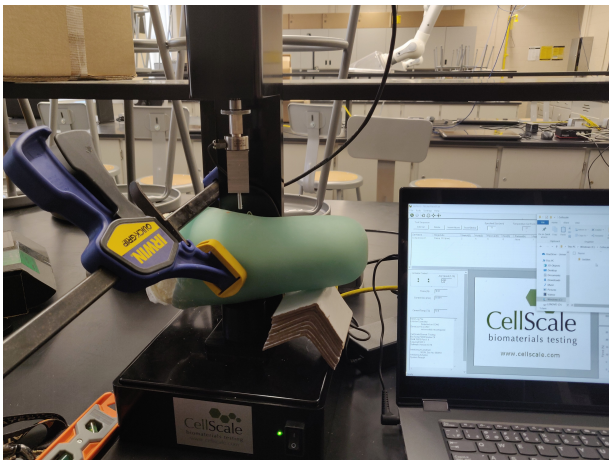

Figure 12: Placement of biofidelic limbs underneath the indenter with clamping setup for popliteal location

Setup of the UTM CellScale testing setup procedure is described as follows:

1. Power on Cellscale UTM system and launch Cellscale Univert desktop application.
2. Reset Actuators (via CellScale app)
3. Set and align limb under indentor with intended location of testing (e.g., fibular head).
4. Ensure limb is level from proximal to distal ends of the limb using a bubble level across the limb.
5. Clamp the limb to the Cellscale using a wood clamp with minimal pressure.
6. Step actuator until Force reading becomes constant (Typically 0.22N).
7. Run cycle test.
8. Repeat 2-7 for each location (i.e., popliteal, patellar, fibular head).

Relaxation testing was performed using the general testing speed and parameters described in steps 1-6, with the exception of initial position and cycle time. In contrast with the loading protocol, each cycle was held in the 10mm position and the change in force was recorded for 120s in the relaxation protocol. In Figure 13, the displacement profile used to achieve the relaxation curves is illustrated. As seen, a displacement of 10 mm was used and held for 120s before releasing.

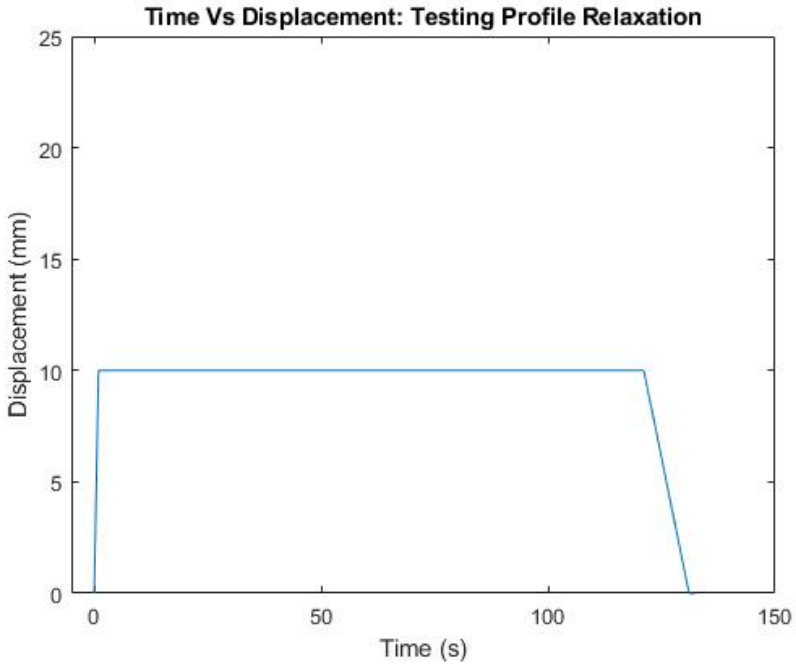

Figure 13: Time Vs Displacement relaxation profile used for testing

Sizing was also measured for each limb in both the virtual model and the 3D printed biofidelic limbs for all sizes tested. The measurements were taken 20mm from the distal end and 50mm below the tibial tuberosity. The height from the tibial tuberosity and distal end were also recorded for each sized limb. All in vivo measurements were taken with a set of calipers across the diameter.

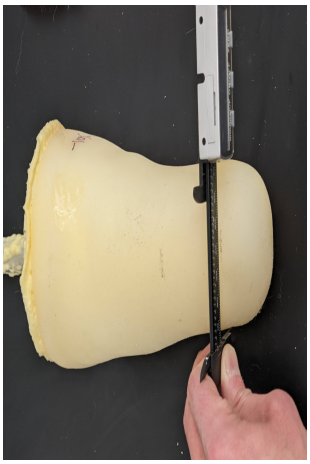

Figure 14: Measurement method for in vivo measurements for biofidelic limbs

3.2.4 Analysis

Once the force, deflection, and time data was exported via .CSV and imported into MATLAB (Matlab R2020a, Mathworks Inc., Natick, MA, USA) via the 'xlsread' function. The relaxation data was plotted as a Force vs Time graph. The force displacement data taken for each zone and limb at 10 cycles was recorded and the poly-fit of these 10 curves were taken with a third order polynomial to calculate the average poly-fit coefficients that were then used to compare to Silver-Thorn. The relaxation data for each data set was used to calculate the % Relaxation at 5s and the total % Relaxation. This was done by using indexing to find the force values at the 5s mark and compared to the Silver-Thorn values found in the same manner. Additionally the force values at 100% relaxation were measured visually by taking the force values where the slope was close to 0.

3.3 Results

Size Control

Measurements from each limb are summarized below with their respective standard deviation and standard error of the mean values for both the in vivo and virtual measurements of the 3D models.

Limb Measurement From Biofidelic Limbs (in mm)			
Location	***Size***		
	-10%'	Regular	+10%'
5cm below tibial tuberosity (Diameter)	73.8	78.8	95.5
2cm above distal end (Diameter)	71.4	81.8	87.8
Height from tibial tuberosity to distal end	136	136	143

Table 1: Data for in vivo measurements using calipers at the tibial tuberosity and distal end locations

Limb Measurement From Mesh Models (in mm)			
Location	***Size***		
	-10%'	Regular	+10%'
5cm below tibial tuberosity (Diameter)	72.7	79.1	89.4
2cm above distal end (Diameter)	68.9	76.3	81.3
Height from tibial tuberosity to distal end	148.5	149	147.6

Table 2: Data for virtual 3D model measurements at the tibial tuberosity and distal end locations

The largest variances that can be seen between the in vivo and virtual measurement are the height measurements and the measurements taken for the +10% limb. The differences in the height are in the range of 4.6-13 mm between the virtual and in vivo measurements. Whereas the difference in the distal end and tibial tuberosity measurements of the +10% limb were 6.5 and 6.1 mm respectively between the virtual and in vivo measurements.

3.3.1 Load Deflection

Raw data from the Cellscale indentation cycles can be seen below in figure 15.

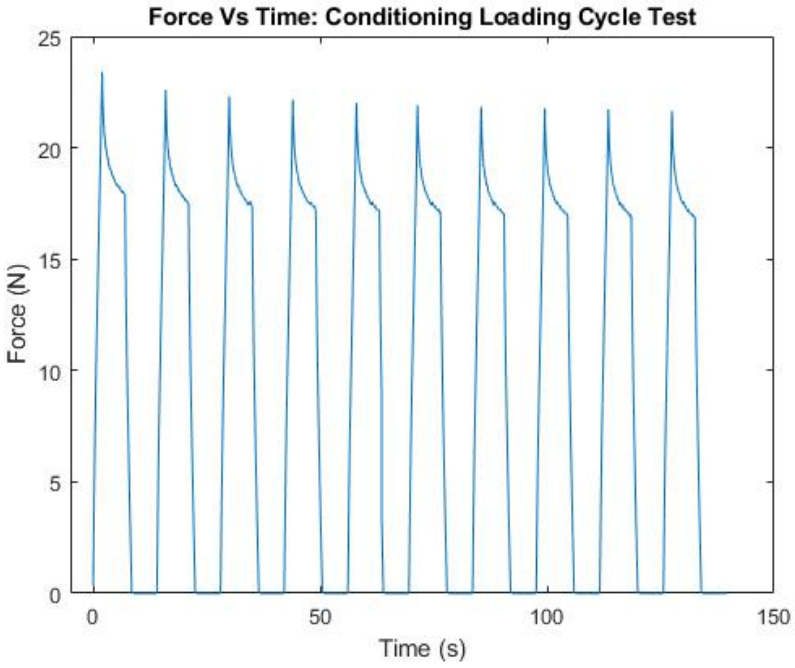

Figure 15: Force Vs Displacement 10 load cycle

It can be seen that the indentation cycles have a noticeable variation from the first to the second cycle in the force peaks, then settles to a relatively steady behaviour. Similarly, the same behaviour is observed in the Force vs Displacement graph in Figure 16 with the first cycle appearing separate from the others.

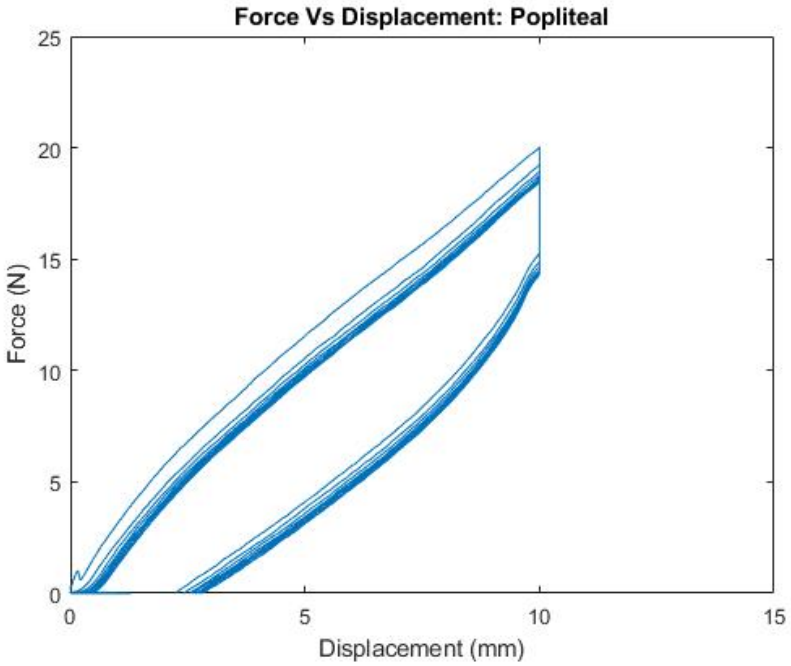

Figure 16: 10 cycle test in the Politeal location (Force Vs Displacement)

Post processed and polyfitted data can be seen below for each of the 10 cycle tests for the Fibular Head, Fibular Head -10%, and Popliteal limb zones in Figures 17-19, respectively.

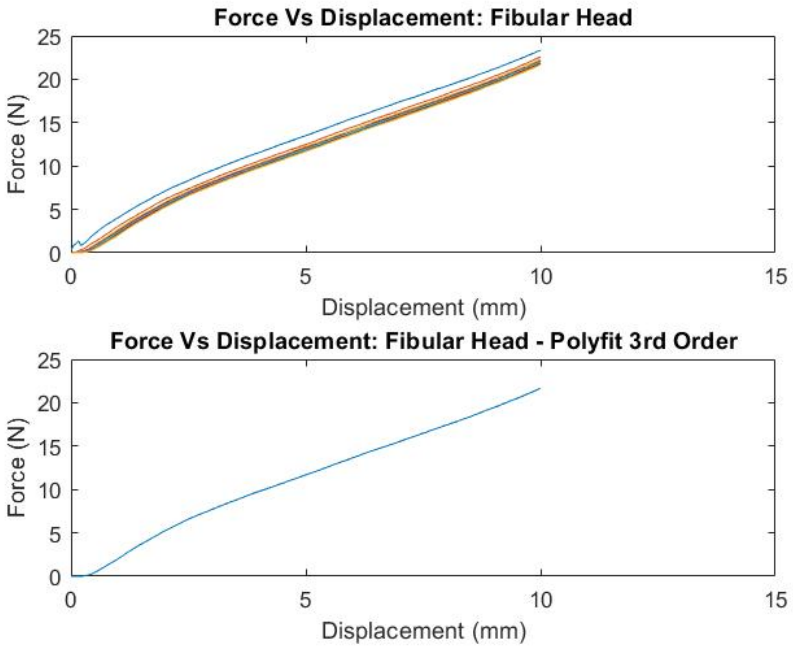

Figure 17: 10 cycle test with a polyfit in the Fibhead location for the regular sized limb (Force Vs Displacement)

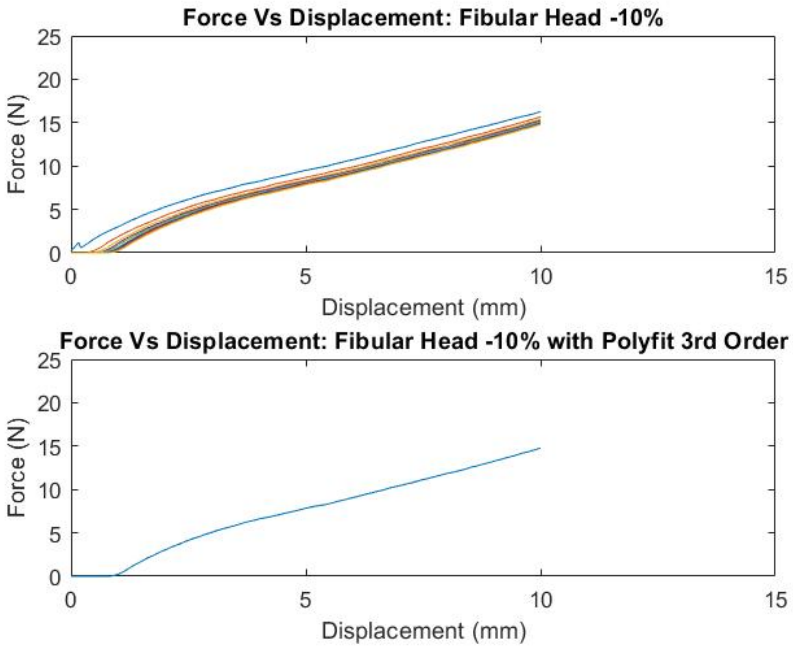

Figure 18: 10 cycle test with a polyfit in the Fibhead location for the -10% sized limb (Force Vs Displacement)

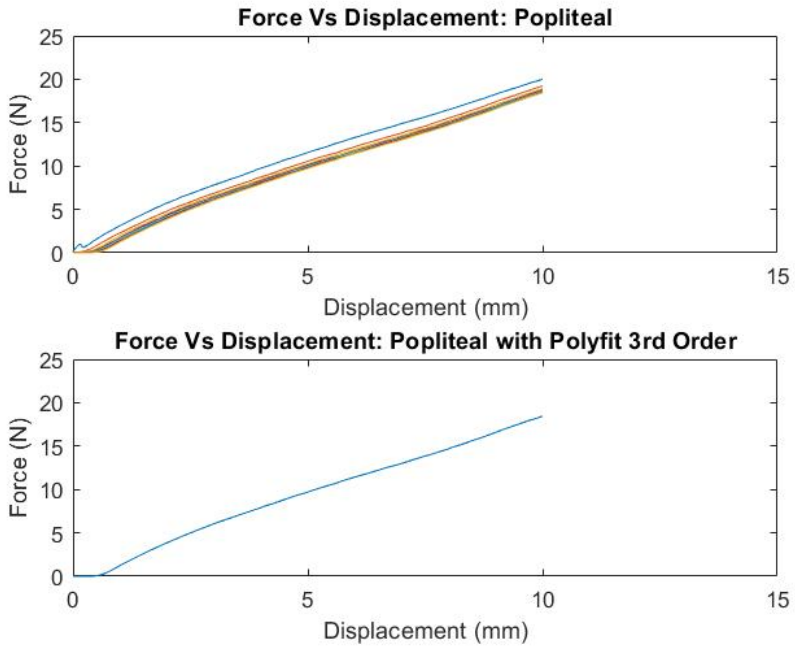

Figure 19: 10 cycle test with a polyfit in the Popliteal location for the regular sized limb (Force Vs Displacement)

The maximum force data from all limb locations is summarized in Table 3. Maximum forces at locations with a smaller thickness of foam between the inserted rod and 3D printed shell, such as the fibular head and patellar zones, exhibited higher max force than the popliteal location. Additionally, the smaller limbs consistently exhibited lower maximum forces.

Max Force Readings (Force vs Displacement)					
Fibhead	*Fibhead -10%*	*Patella*	*Patella -10%*	*Popliteal*	*Popliteal -10%*
23.4	16.3	22.5	16.1	20.1	18.5

Table 3: Max Force Vs Displacement Curves

The summary of the polyfit coefficients for each location and limb can be seen in Table 4. These values will be compared to published polyfit coefficients estimated from in vivo indentation testing [4].

Polyfit Data Coefficients				
	L0	L1	L2	L3
Fibhead-Regular	0.0118	-0.2307	3.3653	-0.776
Fibhead-Small	0.0065	-0.1362	2.2795	-1.0027
Patella-Regular	0.0094	-0.1966	3.1922	-0.9195
Patella-Small	0.0147	-0.2649	2.7509	-0.6967
Popliteal-Regular	0.0061	-0.1264	2.575	-0.8273
Popliteal-Small	0.0071	-0.1108	2.1442	-0.583

Table 4: Estimated polyfit coefficients by location and limb size

3.3.2 Relaxation

In Figures 20-21, the relaxation tests can be seen for the regular and small sized limbs with the patella and popliteal regions.

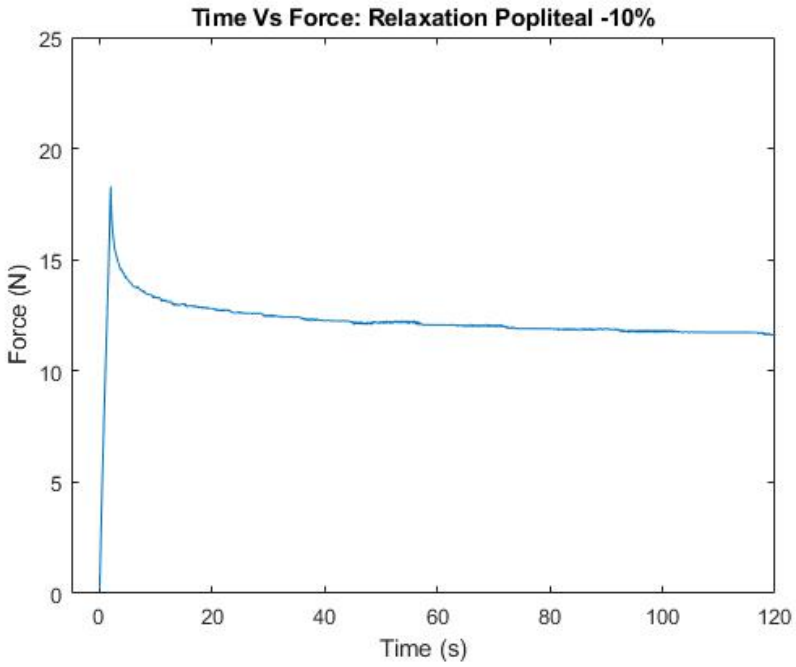

Figure 20: Force Vs Time Relaxation Curve Popliteal -10%

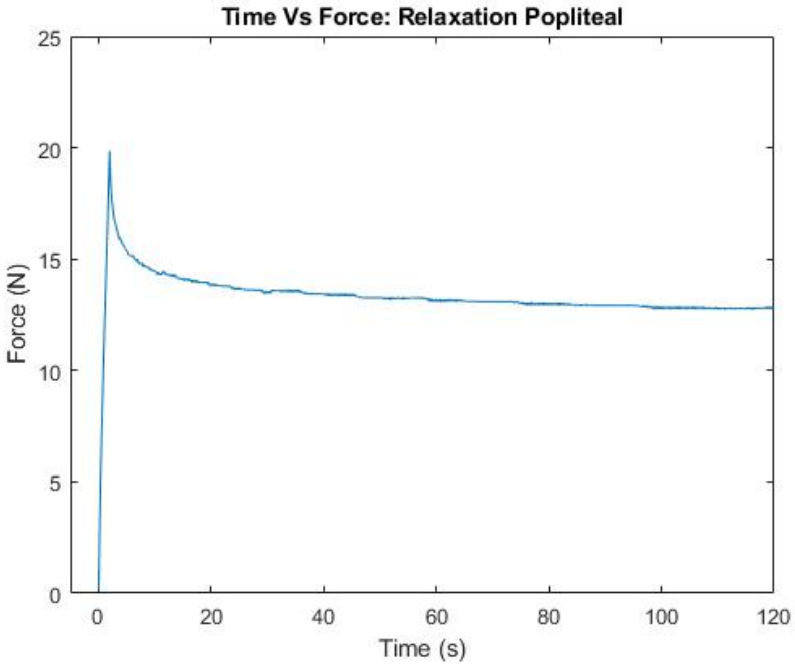

Figure 21: Force Vs Time Relaxation Curve Popliteal - Regular

Maximum forces recorded in relaxation testing is summarized in Figure 26. Relaxation tests on the popliteal and popliteal -10% regions showed little difference in the maximum force. However, differences were observed between maximum forces on the patella (24.9N) and patella -10% (17.5N). At the popliteal location, the popliteal reached 19.9N maximum force and the popliteal -10% reached 18.3N. At the patella, less initial relaxation than its -10% counterpart was observed, with 9.51% less relaxation at 5s whereas the popliteal experienced only 0.07% less than its -10% counterpart at the 5s mark. The relaxation data is summarized in Tables 5 and 6.

Max Force Readings (Relaxation)			
Patella	*Patella -10%*	*Popliteal*	*Popliteal -10%*
24.9	17.5	19.9	18.3

Table 5: Max Force of Relaxation Curves

Relaxation Values				
	Patella	*Patella -10%*	*Popliteal*	*Popliteal -10%*
5s Relaxation (%)	22.43%	31.94%	22.67%	22.74%
Total Relaxation (%)	37.05%	39.06%	35.47%	29.89%

Table 6: Relaxation Values

3.4 Discussion

In this chapter, a method of fabricating biofidelic residual limbs capable of meeting geometric shape and material properties was described. The method comprises of optical scanning of residual limb molds generated by a prosthetist, 3D printing a flexible outer 'skin', and a foam product simulating soft tissue around an aluminum 'bone'. Using mesh manipulation tools to simulate limb volume change, a set of 3 limbs of varying size (-10%, Regular (or full-size), +10%) were generated. The fabricated limbs were tested using a rate-controlled indentor to measure the material characteristics compared to data reported by Silver-Thorn, 1999 [4].

3.4.1 Size Control

There were inconsistencies, seeing a maximum of 13mm height difference between the 3D model and in the resulting product for all sized limbs. Additionally a maximum diameter of 6.5mm difference was seen for the +10% limb between the virtual and in vivo models. This showcases potential problems with the larger models in particular but also an issue of correct height dimensions of limb modelling.

3.4.2 Constant speed

As shown in Figures 17-19, fairly consistent results were observed between locations with few changes in profile during 10 mm/s indentation testing. The forces between these graphs are the largest differences that can be observed within the raw data. Silver-Thorn reports significant variations across different locations since human tissue will have significantly greater variances in material characteristics due to bone location, tissues formations, tissue interactions (visco-elasticity) and other factors. However, in the case of Silver-Thorn these changes were large, ranging from 10 to 45N depending on the location on the same subject. In contrast the data here only shows a max difference of 3.36N between locations. This point to the fact that limb thickness across the foam, skin, and bone layers are too uniform and should have more variation to them especially in areas with bony prominence's like that of a tibial area. It should also be noted that the 10 cycle testing showed that little change was seen to justify removing the first three cycles as seen in Silver-Thorn[4].

Additionally, the polyfit coefficients match closely for L0 and L1. L0 and L1 in our testing resulted in values ranging from 0.0061 to 0.0118 and -0.1108 to -0.2307 respectively whereas in Silver-Thorn these were reported ranges in the -0.03 to 0.05 and -0.19 to 0.81 range for the 10mm/s testing. However, due to the complexity of human tissue, particularly in amputees, likeness varies as the indentation force interacts with other tissues and bone interactions to create an exponential curve as seen in Silver-Thorn, 1999 [4].

AMPUTEE SUBJECTS	L_0	L_1	L_2	L_3
Overall (n=149)	0.01 ± 0.03	0.28 ± 0.45	-0.24 ± 1.54	0.93 ± 1.17
Overall - $\lvert L_i \rvert$ (n=149)	0.02 ± 0.03	0.37 ± 0.38	1.07 ± 1.13	1.06 ± 1.05
1 mm/s (n=51)	0.02 ± 0.02	0.23 ± 0.38	0.19 ± 1.03	0.53 ± 0.76
5 mm/s (n=50)	0.00 ± 0.03	0.31 ± 0.47	-0.45 ± 1.71	1.12 ± 1.27
10 mm/s (n=48)	0.01 ± 0.04	0.31 ± 0.50	-0.46 ± 1.71	1.15 ± 1.30

NON-AMPUTEE SUBJECTS	L_0	L_1	L_2	L_3
Overall (n=30)	0.13 ± 0.09	-0.41 ± 0.59	1.85 ± 1.73	-0.72 ± 1.27
Overall - $\lvert L_i \rvert$ (n=30)	0.13 ± 0.09	0.50 ± 0.52	1.94 ± 1.63	1.05 ± 1.00
3 mm/s (n=10)	0.06 ± 0.04	-0.15 ± 0.31	1.14 ± 0.92	-0.11 ± 0.56
5 mm/s (n=10)	0.16 ± 0.07	-0.65 ± 0.60	2.80 ± 1.70	-1.50 ± 1.23
9 mm/s (n=10)	0.17 ± 0.11	-0.42 ± 0.72	1.62 ± 2.06	-0.54 ± 1.50

Figure 22: Polyfit Coefficients From Silver-Thorn Indentation Testing [4]

3.4.3 Relaxation

The relaxation data in Silver-Thorn [4] ranges from 25.35-49.25% at 5s which matches closely to the 22.43-31.94% found in the biofidelic limbs. However, at full relaxation the biofidelic limbs achieve a 29.89-39.06% relaxation whereas in Silver-Thorn [4] it is reported as 43.51-68.03%. The relaxation data showed a stiffer response in the biofidelic limbs compared to reported human responses. While the biofidelic limbs offer a good foundation, there is more complexity required to achieve true biofidelity. Adding fibular and tibial bone geometries to the models, as well as refining materials to be more visco-elastic may improve the characteristic response to achieve a more exponential curve as seen in Silver-Thorn for the constant speed testing as well as closer values to the reported full relaxation [4]. The geometric profile and characteristics of the limb will have a large effect on how the limb reacts dynamically, how the limb reacts in specific locations, and assessing skin health safety.

Amputee Subjects	Site	$d_{applied}$ (mm)	F_{max} (N)	E_R (N/mm)	τ_ε (s)	τ_σ (s)	% Relaxation Overall	%Relaxation 0 to 5 sec
A1	1	7.5	11.3	1.06	33.58	43.05	29.71	11.65
	2	8.0	4.1	0.29	34.22	45.62	43.43	31.20
	3	5.0	3.8	0.50	13.50	16.86	33.02	25.37
	4	5.5	7.9	0.45	28.50	49.58	68.62	49.12
	5	4.3	1.8	0.21	73.54	102.25	49.93	26.69
	6	6.2	2.9	0.20	32.41	51.95	56.30	37.37
	7	4.0	1.1	0.12	48.81	71.28	57.95	38.70
	8	6.0	9.1	0.81	17.37	25.13	46.61	29.77
	9	4.5	2.2	0.24	74.95	101.14	50.21	36.26
	10	4.0	1.3	0.15	19.84	28.08	53.68	41.56
	11	5.8	11.3	0.63	30.60	55.24	67.56	51.31
A2	2	2.2	7.4	1.27	45.10	79.67	58.89	29.35
	3	3.0	1.0	0.12	6.03	10.93	61.76	44.85
	6	2.6	1.0	0.14	8.08	13.94	61.42	49.97
	8	2.7	6.4	1.30	81.97	118.12	44.61	32.30
	9	3.0	4.7	0.45	29.52	78.60	71.00	37.99
	11	2.7	3.0	0.58	31.19	44.20	47.41	28.12
A3	1 - 11			N/A	N/A	N/A	N/A	N/A
A4	1	6.5	4.3	0.38	11.88	16.90	41.85	25.26
	2	5.0	3.1	0.27	54.77	97.16	56.38	24.70
	3	4.5	1.5	0.09	50.35	110.49	73.28	56.43
	4	5.2	0.7	0.04	5.59	14.22	68.23	45.36
	5	5.8	2.8	0.28	48.37	59.48	43.17	29.07
	6	6.0	5.3	0.46	29.54	44.54	48.33	26.22
	7	2.5	22.0	1.85	23.98	88.32	78.97	36.37
	8	3.0	0.5	0.04	459.01	610.96	79.41	76.58
	9	4.5	1.8	0.23	11.07	16.24	43.35	31.68
	10	5.0	0.7	0.02	30.98	107.03	82.58	47.34
	11	7.0	2.3	0.13	33.66	61.69	59.59	30.22
A5	1	3.5	2.9	0.34	8.15	15.62	58.25	37.63
	2	9.0	2.5	0.15	10.93	15.37	46.60	35.99
	3	8.0	6.7	0.33	37.59	59.58	60.79	40.50
	4	3.0	0.9	0.13	10.05	16.55	54.72	45.27
	5	5.0	4.2	0.43	58.06	95.51	49.24	21.50
	6	6.0	3.0	0.21	10.52	22.53	58.19	28.48
	7	3.0	1.0	0.13	20.15	32.46	58.35	51.45
	10	5.5	2.6	0.24	40.61	53.21	48.68	48.29
	11	6.3	3.7	0.28	18.43	26.38	51.38	40.04
	Mean	4.9	4.1	0.39	*42.78*	*67.56*	*55.77*	*37.30*
	S.D.	1.7	4.1	0.40	*73.09*	*97.50*	*12.26*	*11.95*

Figure 23: Max Force and Relaxation Data from Silver-Thorn

3.5 Conclusion

In this chapter, an artificial residual limb with biofidelic geometry was developed and tested. Mechanical testing was conducted and compared to published in vivo data to characterize the biofidelic limb properties. In constant speed indentation tests, the proposed biofidelic limbs demonstrated comparable responses to published in vivo values. Futhermore, these responses were consistently observed at all locations tested. Relaxation data indicates significant differences in visco-elastic properties. Overall, these findings indicate good mechanical properties under steady-state or quasi-static (i.e., slow) mechanical loading stimuli. Further development is needed to offer biofidelic dynamic mechanical responses.

4 Fit Sensing for Biofeedback

4.1 Introduction

Many of the problems associated with poor fit for lower limb amputees stems from neuropathy[21][13], which impairs the nerves in the lower limbs and causes numbness or loss of feeling entirely. This leaves the amputee with deficits in tactile sensation, including sensing the socket interface pressure[13], temperature, humidity, discomfort, and/or pain[22]. Coupled with fluctuations in residual limb volume varied by activity, hydration, inflammation, diet, and other factors, a system to provide fit feedback and guide amputees on lower limb maintenance is needed[8].

When an amputee loses significant residual limb volume, a phenomenon called sinking occurs where the residual limb sinks down into the socket through gravity. Sinking causes pistoning, where the residual limb exhibits a loss of suction in the socket allowing movement vertically, which may result in discomfort, gait problems, and high risk of pressure sores[5]. To address lack of tactile sensation associated with neuropathy, a proposed solution is to apply a sensor system at the distal end of the socket interface in a biofeedback approach. Upon detection of sinking, a reminder or notification system can prompt users to inspect and maintain limb health. In accordance with self-management programs, triggered notifications can inform the user of sinking, prompt the user to add a sock, and to check limb health (e.g., visual inspection of the skin). In this Chapter, the sensor concept was tested using the biofidelic limbs simulating volume changes towards validating the sensor system's capabilities.

This Chapter presents development of a pressure sensor embedded into the distal end of the socket to capture volume changes. While few socket fit sensors currently exist, the most widely used fit measurement system inside a prosthetic socket is a system of force sensitive resistance sensors (FSRs) that creates a pliable film that can be custom fit to various profiles. As a research tool, the F-socket system (Tekscan, Inc., Boston, Massachusetts, United States) has been used extensively in the scientific literature to detect changes pressure around the socket walls [23]. However, the F-socket system (Tekscan, Inc., Boston, Massachusetts, United States) is limited due to the resource-intensive setup for measurements, high cost (approx. $25,000 USD) making it unaffordable for most prosthetic users, and signal drift, hampering actual use with a patient over long periods. To design an improved sensor system it not only needs to minimize cost but is also required to not affect the socket-limb interface, be easily integrated into a socket fabrication workflow, and low maintenance. Specifically, the objectives of the chapter are to describe the design process, including the placement and type of sensors, report fabrication methods aligned with current workflow, and evaluate the ability to detect volume or fit changes.

4.2 Methods

The overall goal of the current Chapter is to develop and test a socket sensor system capable of detecting fit changes associated with residual limb volume change.

4.2.1 Specific Goals/Objectives:

The goals and objective for the biofeedback system in this chapter are to:

1. Design a biofeedback system comprising of sensor(s), datalogging, and notifications/visualizations for user feedback.
2. Develop fabrication methods appropriate to current socket manufacturing processes
3. Evaluate system performance to indicate fit using the biofidelic limbs generated in Chapter 3
4. Characterize the relationship between sensor output (pressure) and limb volume, including constant force and settling time following unloading
5. Investigate settling time after applying constant force to system for each of the inserts.
6. Investigate settling time after removing input (constant force) to the system (time it will take sensor output to reflect zero force applied to system), for each of the inserts.

4.2.2 Biofeedback system design

Electronics Software

The system electronics consist of: sensor(s) components, Bluetooth wireless data transmission, and power infrastructure. Several sensors were investigated including a fabric-based capacitive sensor (StretchSense, Penrose Auckland, New Zealand), a force-sensitive resistor sensor (SingleTact, Medical Tactile Inc, Los Angeles California, USA), and a pneumatic sensor (PicoPress, Medi-Group Micro Labs, Sydney, Australia). These sensors were tested briefly based on compatibility with current socket fabrication methods, and sensor drift.

The StretchSense detects stretching or bending stimuli in a flexible, fabric medium. Mounting design concepts were difficult to incorporate into socket designs balancing limb interactions to stimulate the sensor with standard socket fabrication methods. The candidate FSR-based Singletact sensor demonstrated significant drift tested using a calibration weight for 8 hours, a known issue with FSR technologies.

Thus the pneumatic sensor, PicoPress, was selected due to its lack of drift and ease of incorporation into the socket fabrication process. Shown in Figure

31, the PicoPress is a closed pneumatic system comprised of a bladder connected to 3.98 mm diameter tube which was plugged into a valve and pressure transducer (Model:TBP-D-AN-N-100MG-U-C-V from Honeywell International Inc. in Charlotte, North Carolina, USA). Measuring pressure changes inside the closed system through the tubes caused by the compression of the bladder component interfacing with the limb. The pressure transducer is connected to the input of a Bluno Nano (Model: RB-Dfr-572 from Arduino in Somerville, MA, USA) to acquire and wirelessly stream digital pressure signals to a Bluetooth-connected device.

Raw signals sent to a Bluetooth-enabled device (Pixel, Google Inc., Mountainview, CA, USA) were processed and displayed in a meaningful manner to the user. A basic Android OS app was created for testing and data processing purposes, enabling basic data streaming, logging, and visualization functions on the mobile device. Data, collected at a rate of 10 Hz (100 ms period), was stored as a text (.csv) file locally on the device. Additionally this data can be processed and displayed in an app to provide useful fit data - a prototype mobile app was developed by a 4th year project team called Augeo Medical which can be seen below [24].

Figure 24: Mobile App Prototype for Fit Feedback

All devices in the system were powered via a 5v USB connection.

4.2.3 Fabrication

Since the socket has a fragile interface, it is crucial that the sensor does not disrupt the limb-socket interface. Since the PicoPress is an air-filled bladder, sensor mounting presented a technical challenge. With over 20 years of prosthetics fabrication service experience, Prosthetic Ability (Kitchener, ON, Canada) is a local orthotics provider partnering with our research group to provide clinical feedback. Considering their existing workflow, methods to create negative space in the socket for the component to sit into were generated and tested in an iterative manner.

During the process of creating a lower limb socket, the orthotist commonly creates a negative space during the casting process for placement of relief valves and/or ports. This is achieved using a "dummy" silicone tube of the desired size inserted into the malleable (heated) thermoplastic before curing takes place. The soft thermoplastic material cures around the tube, which can then be removed to expose the negative space. To create a dummy for the PicoPress bladder, a PicoPress bladder was first casted in a plaster mold. The resulting dummy was used to create a negative space in the distal end of the socket. Not only is the mounting method consistent with existing socket manufacturing processes, the process requires about 10 mins of extra labor and does not lead to significantly increased fabrication costs to install the proposed biofeedback system.

4.2.4 Testing

To confirm that the volume changes in the biofidelic limbs can be detected by the distal end PicoPress sensor, validation of the sensor's capabilities to measure changes in volume was conducted. The goal of this testing was to characterize the effects of lower limb volume changes on PicoPress pressure signals. A secondary goal was to characterize sensor drift characteristics.

The complete setup for the testing can be seen in the figure below. Briefly, the prototype socket with distal sensor is mounted to a flange. In order to load the system with weight, a platform was fabricated to fit to the rod or "bone" of the biofidelic limbs. The procedure to test the proposed socket sensor system is described below:

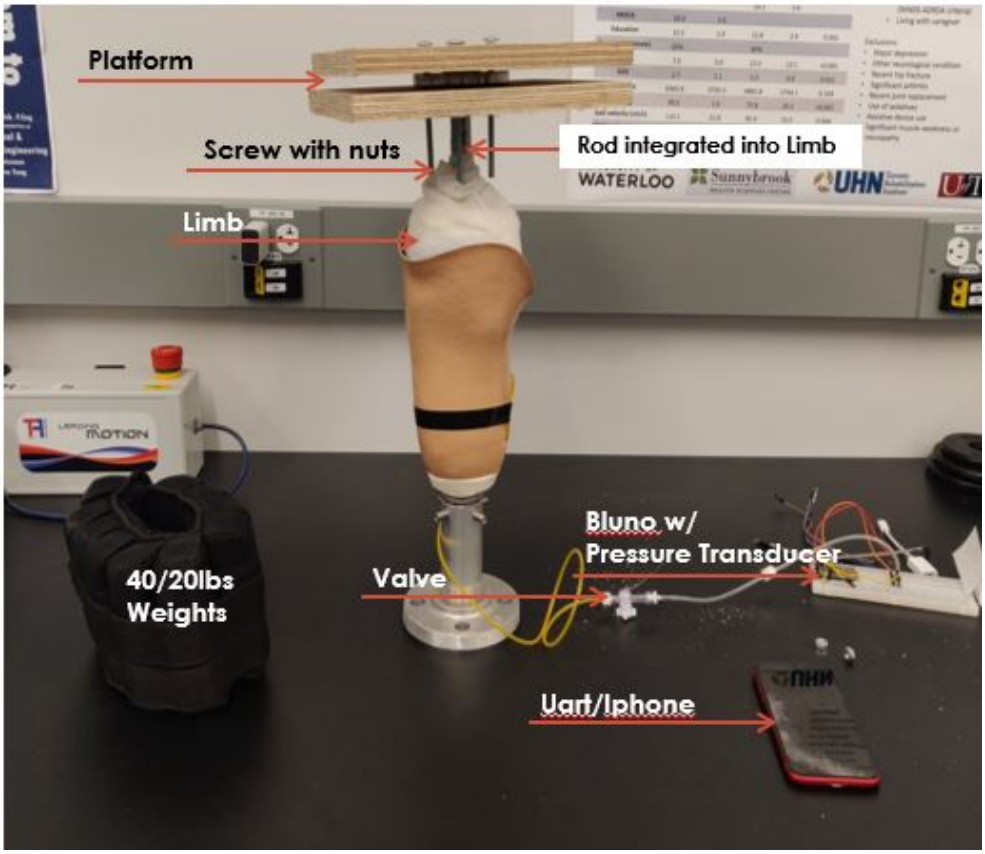

Figure 25: Mechanical Test Setup of the prototype socket sensor

The procedure for this testing is as follows and was repeated 15 times for each size limb insert:

1. Place insert into socket. Ensure it is well mounted for proper fit. Begin datalogging with mobile device
2. Ensure the plate atop of the insert is mounted flat
3. Measure unloaded output pressure reading
4. Place weight atop of flat plate and begin timer. In this test, weights of 20 and 40 lbs (9.07 and 18.14 kg) were employed
5. Once output pressure readings have settled to consistent readings, remove the weights from the plate
6. Monitor pressure versus time relationship to capture settling times for both the input applied (Step 5) and once removed (Step 7)

7. Remove the top plate from the insert. Then, remove the insert from the socket. Continue recording until sensor readings have settled to a stationary state

8. Repeat procedure for 15 trials with a single limb size

The procedure was conducted for the small (-10%), regular and large (%) biofidelic limbs. The order of trials were randomized to ensure that results were not affected by a specific sequence of inserting the limbs during testing.

4.2.5 Analysis

Once the data was collected, records were exported (to .CSV) and imported to MATLAB (via Matlab function 'csvread'). The data was then smoothed using Matlab function 'smooth' with a 7.5% span of data points and the 'loess' function. 'Loess filter', a non-parametric smoothing function that does not assume a predetermined shape, was chosen due to the limited number of outliers present which will greatly affect the outcome of loess smoothing. Each data set contain 10 sets of data, as shown superimposed in Figure 26. To align the starting points of all the graphs, a phase shift was applied to each trial (not shown). In order to examine the relationship between limb size and PicoPress pressure, the plateau (or flat) regions of the curves were determined and averaged across trials. For each trial, the center point of the plateau was determined and averaged across all ten tests, and conducted across regular, -10% and +10% limb tests.

4.3 Results

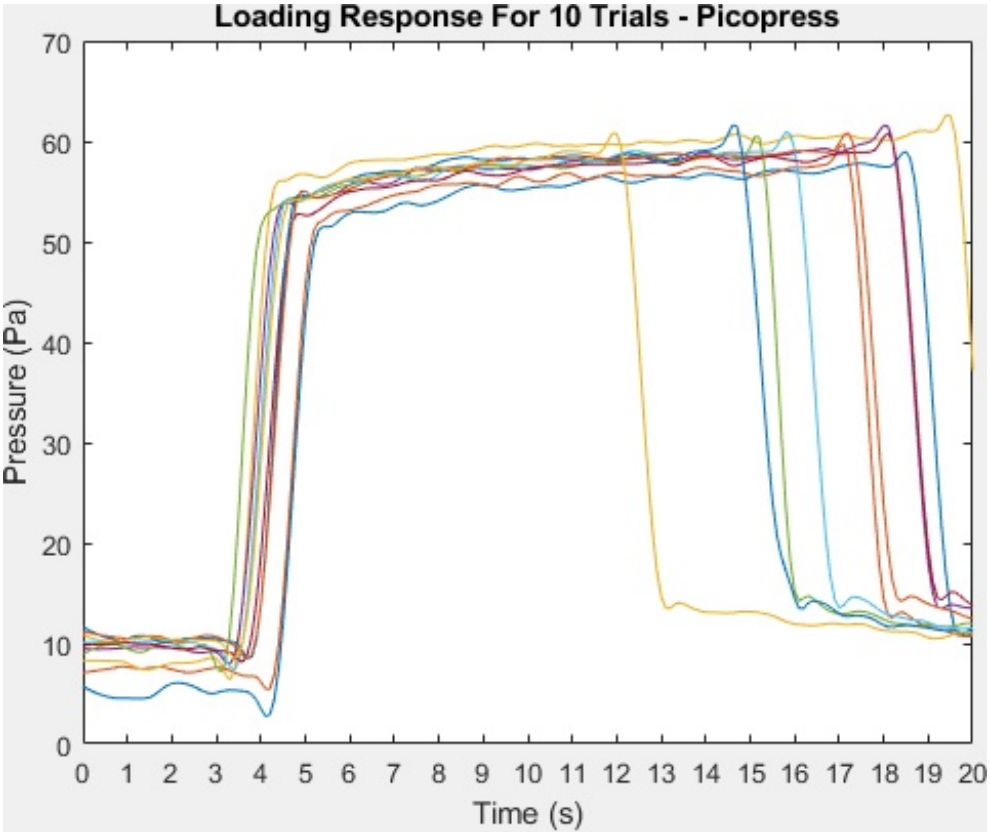

Figure 26: Pico-Press Validation Data on Regular Sized Limb Using Weighted Biofidelic Limb Procedure

As shown in Figure 26, the Regular (Full-size) limb yielded a mean (+/-STD) pressure of 57.54 +/- 0.38 Pa in the plateau region.

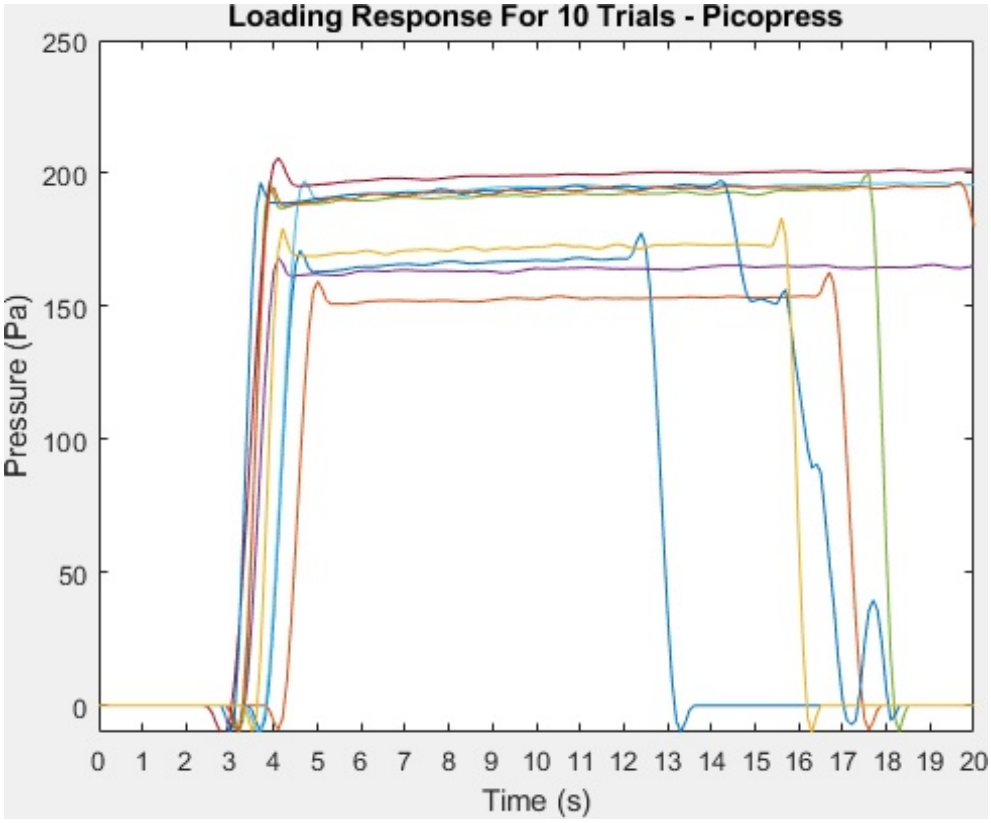

Figure 27: Pico-Press Validation Data on Small Sized Limb (-10%) using Weighted Biofidelic Limb Procedure

The small (-10% of Regular size) limb, shown in Figure 27 resulted in a mean (+/-STD) pressure of 179.61 +/- 5.44 Pa during the plateau region.

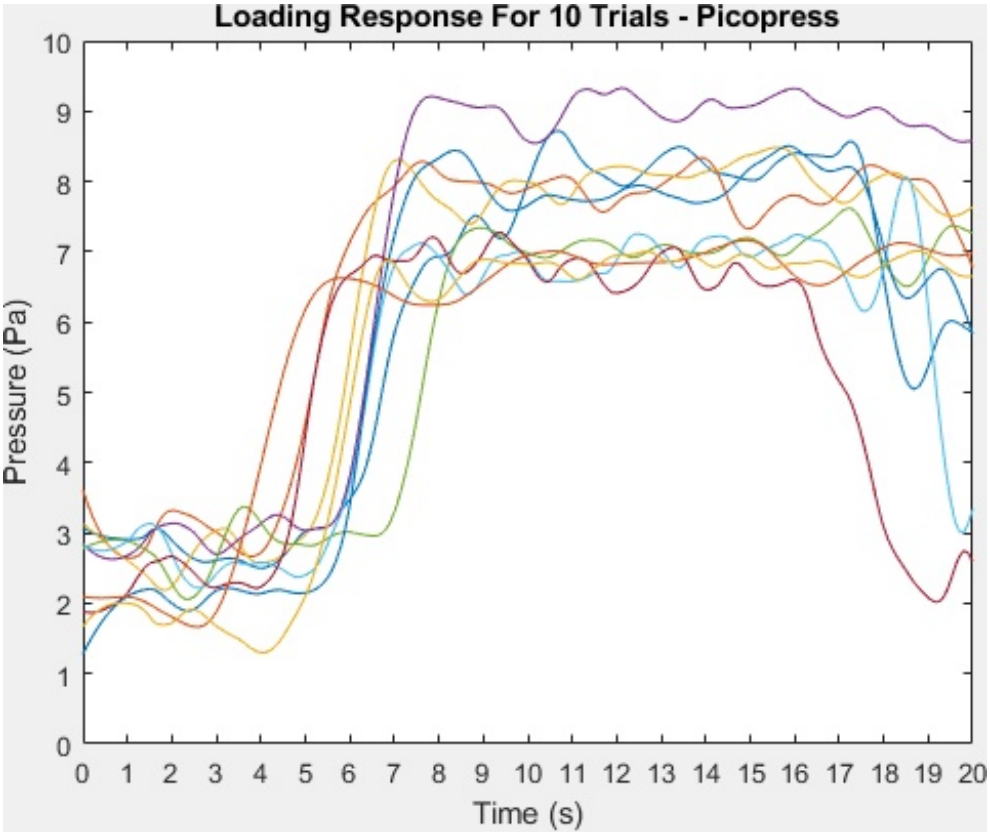

Figure 28: Pico-Press Validation Data on Large Sized Limb (+10%) using Weighted Biofidelic Limb Procedure

The large (+10%) limb showed a mean (+/-SEM) pressure of 7.57 +/- 0.25 Pa during the plateau region as seen in Figure 28.

In general, the PicoPress pressure responses were fairly consistent with standard deviations < 0.4 Pa in the regular and large limbs. In the smaller (-10%) limb testing, variations were larger (STD=5.4 Pa) in the pressure values and were observed to have changes as high as +/- 50 Pa.

In Figure 29, the settling time data is summarized where the average settling time increases with the size of the limb ranging from 1.14s, 1.28s and 3.12 s respectively for the -10%, Regular and +10% limbs respectively. The Standard Deviation and Standard Error of the Mean were observed to increase as the limb size went smaller.

Settling Times for Pico-Press Data			
Limb Size	***Average***	***ST.Dev***	***SEM***
Regular	1.278	0.109	0.012
-10%'	1.144	0.194	0.022
+10%'	3.122	0.148	0.016

Figure 29: Settling times calculated for various sized limbs testing the mechanical testing setup and weight protocol with respective standard deviation and standard error of the mean

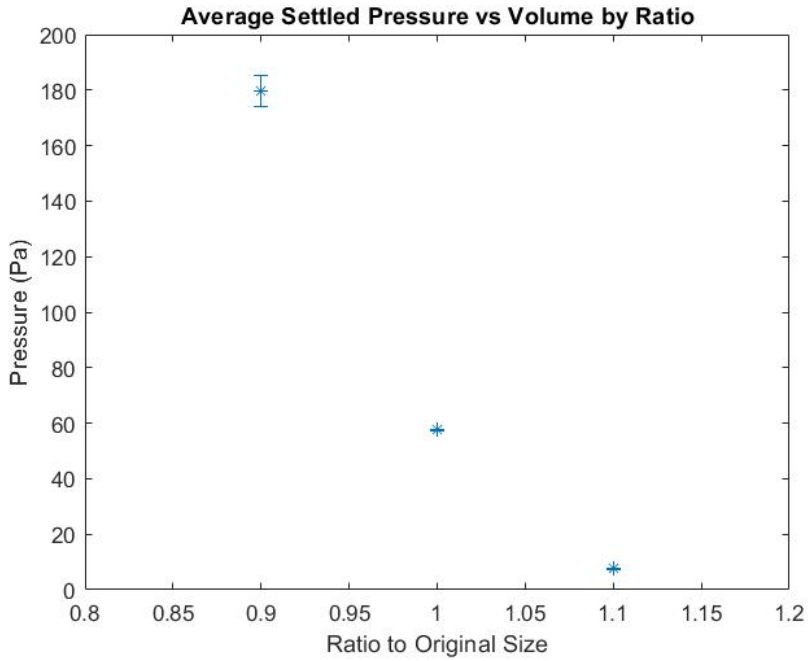

Figure 30: PicoPress mean (and standard error) output values by limb size (expressed as a ratio).

Mean (and standard error) PicoPress pressure values plotted as a function of limb size ratio in Figure 30. Distal end pressures indicated by the PicoPress sensor were highest in the small (-10%), followed by the regular size limb. Lowest pressures were observed in the large (+10%) limb.

4.4 Discussion

This Chapter presented development of a pressure sensor embedded into the distal end of the socket to capture volume changes, and testing using a set of biofidelic limbs (described in Chapter 3). Overall, the prototype sensor system met criteria for measuring distal end pressures associated with varying volume and implementation into current socket fabrication practice.

As seen in Figure 30, the prototype sensor system demonstrated promise for use as a solution to detect distal end pressure changes related to volume changes. As expected, the pressure increased as the limb decreased in volume attributable to the 'sinking' phenomenon. With a smaller limb size under loading conditions, the surface area around the limb to provide vertical support decreases, leading to limb compression and 'sinking' inside the socket. Conversely, the larger limb was a tight fit in the socket, resulting in reduced pressures observed at the distal end. This is largely attributable to increased distribution of vertical loads combined with increased shear in the proximal surfaces. While the relative contribution of shear forces is not measured in this chapter, the increased normal forces associated with a tighter fit is likely to lead to greater friction (and shear) at the interface.

Settling time proportionality to an increase in limb size was shown - this will be problematic with dynamic changes for larger users and would need to be addressed so that all users could benefit from the feedback and health monitoring a socket sensor could provide. This would need to be validated with a more robust testing approach since the settling times may be varying due to the manual nature of the test - using a Universal Testing Machine to insert and remove the limb would be a more robust validation method.

Variability in pressure records supports promising reliability for the proposed distal end pressure sensing approach. In Figures 26-28, the data is fairly repeatable and consistent throughout the testing. Largest variations were observed in the small limb, largely attributable to variations in manual insertion and removal of the limbs. Observing the trial pressure traces, peaks can be seen when inserting and removing the limb from the socket, showcasing the sensor's ability to detect the pistoning phenomenon. In figure 27, this "cat ears" effect of the socket being pushed in, released, and pulled out can be clearly observed. In the regular (Figure 26) and larger (Figure 28) limbs, pressures show fairly settled signals in the plateau region with smaller variation compared to the small limb (Figure 27). These findings support the system's ability to detect consistent pressure changes likely to be seen in prosthetic use.

While adequate for preliminary examination of the relationship between limb volume and distal end pressure, the primary limitations of the current Chapter are the limited variation in biofidelic limb shapes and sizes and lack of criterion-standard validation data. Considering limb geometry is a critical factor in pressure distribution across the socket-limb interface, using a single limb geometry limits the generalizability of the reported values. As such, it is likely that relative pressure changes are used to trigger alerts as opposed to absolute pressure values. Furthermore, a limited range of biofidelic limbs with varying

sizes are available. Ideally, rigorous testing across a large range of limbs and sizes would be conducted to examine whether absolute pressure values could be used to determine fit changes. A comparison with a criterion-standard sensor, such as the Tekscan F-Socket system, would be useful to validate the PicoPress capabilities.

4.5 Conclusion

In this chapter, a novel distal end pressure sensor to monitor fit was developed and prototyped. Comprising of a pneumatic (PicoPress) sensor embedded into the socket, the prototype was developed in collaboration with local orthotists experienced in fabricating sockets to meet current practices. Proof-of-concept testing using a set of biofidelic limbs of systematically varying circumference yielded promising results to indicate socket fit conditions, particularly sinking. Overall, the prototype sensor system met criteria such as detecting pistoning (distal end pressures), limb fit changes caused by both increased and decreased volume, as well as being a low cost and simple method of installation for implementation into current socket fabrication practice.

5 Summary of contributions and future Work

5.1 Summary of contributions

In this thesis, a novel method of creating biofidelic amputee limbs was found and validated. The novelty of the limbs were in maintaining the geometry and material responses of a true limb. The 3D printed outer skin method successfully generated limbs with complex geometries representative of in vivo amputees, and a series of limbs ranging from the normal (or full) size to a smaller size of -10% and a larger size of +10% the original radial dimension. Minor adjustments to the fabricated limb size and materials were identified in order for the limbs to match viscoelastic properties of limb tissues in amputees [4]. However, the limb can replicate volume change conditions within the socket, particularly sinking and fit changes.

In Chapter 4, a novel approach to fit change detection was investigated using a single sensor in the distal end. The sensor detected volume changes through pressure transfer within the socket to the sensor, validated using the biofidelic limbs of varying volume. The sinking effect of the small limb was observed as an increase in distal end pressure, with the swelling effect of the large limb observed as reduced distal end pressure. This sensor system showed promising potential for a low cost biofeedback solution that could be used to provide information to orthotists regarding fit, and inform users on maintenance and fit of their prosthetic socket.

5.2 Future work and recommendations

While a good foundation was set for the biofidelic limbs, the limb model scanned and used for this thesis was of relatively uniform shape. Considering atypical or irregular limb shapes are more likely to require specific attention to prevent skin breakdown and maintain device comfort, more realistic interpretation of a true limb like a bony prominence, fatty area, and/or skin flap may be considered for future improvements. To achieve more biofidelic geometries, a composite bone to match that of the tibia and fibula may be considered. Additionally, a more viscoelastic material needs to be investigated as the current response is too stiff. This could be achieved by introducing gel-like material as an additional thin layer along with the polymer based 3D printed material and flexfoam V! layer. Further validation is then needed to justify using these limbs as a tool for quality of prosthetic devices.

The biofeedback system performed well in the detecting of fit changes within the socket interface. However the long settling time of the sensor limits the use to low frequency feedback and is not adequate for dynamic recordings, such as gait. There are several possible explanations for the long mean settling times. Large variability in settling time data observed in Chapter 4, particularly using the larger biofidelic limb, suggests the insertion and loading procotols may need to be more robustly controlled. Considering the larger limb is a tighter fit, we

partially attribute the variability to settling of the limb (and not necessarily the sensor response). This could be improved by testing the sensor with a larger sample size, and using a more robust load method (e.g., universal testing machine). This would reduce the variation in the response output between tests and allow for a controller to be designed to compensate for the overshoot and drop in settling time.

Finally, it would be crucial to move forward doing in vivo testing trials. This would be most beneficial with a further developed biofeedback app system in place to ask users on the benefits of the system and how to the information is presented.

References

[1] Physiopedia, "Lower limb prosthetic sockets and suspension systems — physiopedia,," 2020. [Online; accessed 15-January-2020].

[2] M. R. Safari, P. Rowe, A. Mcfadyen, and A. Buis, "Clinical Study Hands-Off and Hands-On Casting Consistency of Amputee below Knee Sockets Using Magnetic Resonance Imaging," *The Scientific World Journal*, vol. 2013, p. 13, 2013.

[3] Z. Jin, J. Zheng, W. Li, and Z. Zhou, "Tribology of medical devices," *Biosurface and Biotribology*, vol. 2, pp. 173–192, dec 2016.

[4] M. B. Silver-Thorn, "In vivo indentation of lower extremity limb soft tissues," *IEEE Transactions on Rehabilitation Engineering*, vol. 7, no. 3, pp. 268–277, 1999.

[5] J. E. Sanders, R. T. Youngblood, B. J. Hafner, J. C. Cagle, J. B. McLean, C. B. Redd, C. R. Dietrich, M. A. Ciol, and K. J. Allyn, "Effects of socket size on metrics of socket fit in trans-tibial prosthesis users," *Medical Engineering and Physics*, vol. 44, pp. 32–43, 2017.

[6] R. Hanspal, K. Fisher, and R. Nieveen, "Prosthetic socket fit comfort score," *Disability and Rehabilitation*, vol. 25, no. 22, p. 1278–1280, 2003.

[7] P. A. Lazzarini, D. Clark, and P. H. Derhy, "What are the major causes of lower limb amputations in a major Australian teaching hospital? The Queensland Diabetic Foot Innovation Project, 2006 – 2007," *Journal of Foot and Ankle Research*, vol. 4, dec 2011.

[8] J. E. Sanders and S. Fatone, "Residual limb volume change: systematic review of measurement and management.," *Journal of rehabilitation research and development*, vol. 48, no. 8, pp. 949–86, 2011.

[9] P. J. Potter, O. Maryniak, R. Yaworski, I. C. Jones, and B. Ma, "Department of Veterans Affairs Incidence of Peripheral Neuropathy in the Contralateral Limb of Persons with Unilateral Amputation Due to Diabetes," Tech. Rep. 3, 1998.

[10] K. Ziegler-Graham, E. J. MacKenzie, P. L. Ephraim, T. G. Travison, and R. Brookmeyer, "Estimating the Prevalence of Limb Loss in the United States: 2005 to 2050," *Archives of Physical Medicine and Rehabilitation*, vol. 89, pp. 422–429, mar 2008.

[11] "Variables Affecting Amputees ' Reaction to the Artificial Limbs in the Kingdom," vol. 4, no. 2005, pp. 587–599, 2016.

[12] N. Miller, "Biofeedback and visceral learning: clinical applications.," *Ann. Rev. Psychology*, vol. 29, no. 141, pp. 373–404, 1978.

[13] M.-Y. Lee, C.-F. Lin, and &. K.-S. Soon, "Balance control enhancement using sub-sensory stimulation and visual-auditory biofeedback strategies for amputee subjects," 2007.

[14] ISO/TC210, "ISO 13485:2016 Medical devices: Quality management systems, Requirements for regulatory purposes," vol. 3, pp. 1–36, 2016.

[15] A. P. Pathak, M. B. Silver-Thorn, C. A. Thierfelder, and T. E. Prieto, "A rate-controlled indentor for in vivo analysis of residual limb tissues," *IEEE Transactions on Rehabilitation Engineering*, vol. 6, no. 1, pp. 12–20, 1998.

[16] Ming Zhang and A. Mak, "A finite element analysis of the load transfer between an above-knee residual limb and its prosthetic socket-roles of interface friction and distal-end boundary conditions," *IEEE Transactions on Rehabilitation Engineering*, vol. 4, no. 4, pp. 337–346, 1996.

[17] G. Pirouzi, N. A. Abu Osman, A. Eshraghi, S. Ali, H. Gholizadeh, and W. A. Wan Abas, "Review of the socket design and interface pressure measurement for transtibial prosthesis," vol. 2014, 2014.

[18] E. A. Al-Fakih, N. Azuan, A. Osman, A. Eshraghi, F. Rafiq, M. Adikan, and N. A. A. O. My, "The Capability of Fiber Bragg Grating Sensors to Measure Amputees' Trans-Tibial Stump/Socket Interface Pressures," *Sensors*, vol. 13, pp. 10348–10357, 2013.

[19] H. O. S. O. H. S. K. S. Kenji Hachisuka, Koichiro Dozono, "Total Surface Bearing Below-Knee Prosthesis: Advantages, Disadvantages, and Clinical Implications," 1998.

[20] A. C. Laing and S. N. Robinovitch, "The Force Attenuation Provided by Hip Protectors Depends on Impact Velocity, Pelvic Size, and Soft Tissue Stiffness," *Journal of Biomechanical Engineering*, vol. 130, p. 061005, dec 2008.

[21] A. L. Carrington, C. A. Abbott, J. Griffiths, N. Jackson, S. R. Johnson, J. Kulkarni, E. R. Van Ross, and A. J. Boulton, "Peripheral vascular and nerve function associated with lower limb amputation in people with and without diabetes," vol. 101, pp. 261–6, 2001.

[22] H. Nakajima, S. Yamamoto, and J. Katsuhira, "Effects of diabetic peripheral neuropathy on gait in vascular trans-tibial amputees," 2018.

[23] S. Ali, N. A. A. Osman, N. Mortaza, A. Eshraghi, H. Gholizadeh, and W. A. B. B. Wan Abas, "Clinical investigation of the interface pressure in the trans-tibial socket with Dermo and Seal-In X5 liner during walking and their effect on patient satisfaction," *Clinical Biomechanics*, vol. 27, no. 9, pp. 943–948, 2012.

[24] E. L. Anna Dong, Summer Kavan and I. Morgan, "BME461 AUGEO Capstone Final Conference Report," *University of Waterloo Capstone Projects*, p. 60, 2019.

Appendix

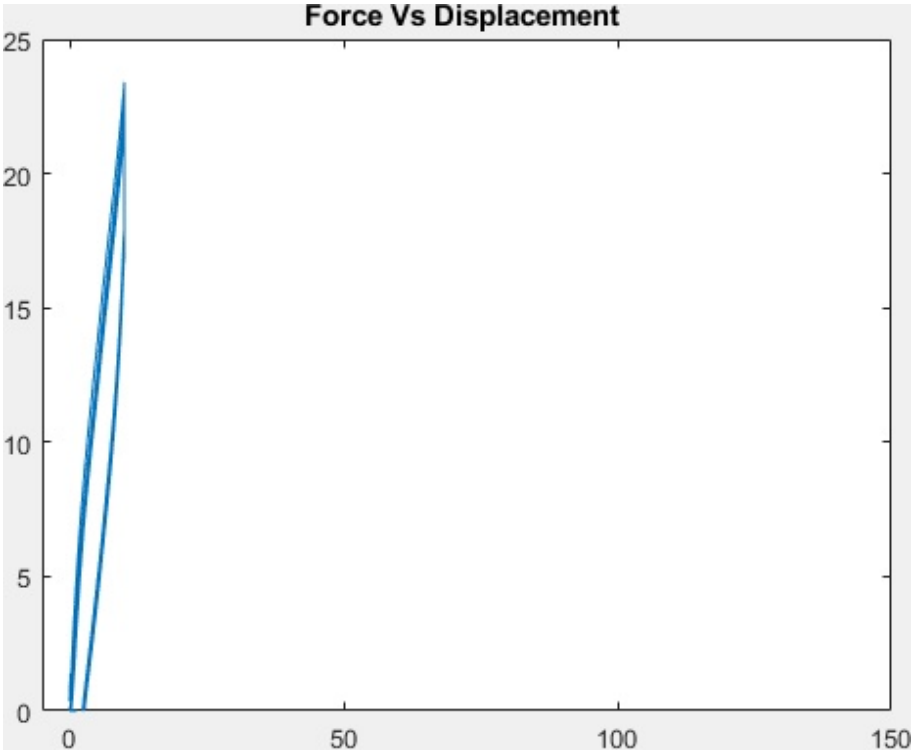

Figure 31: Pressure Vs Displacement 10 load cycles fibhead

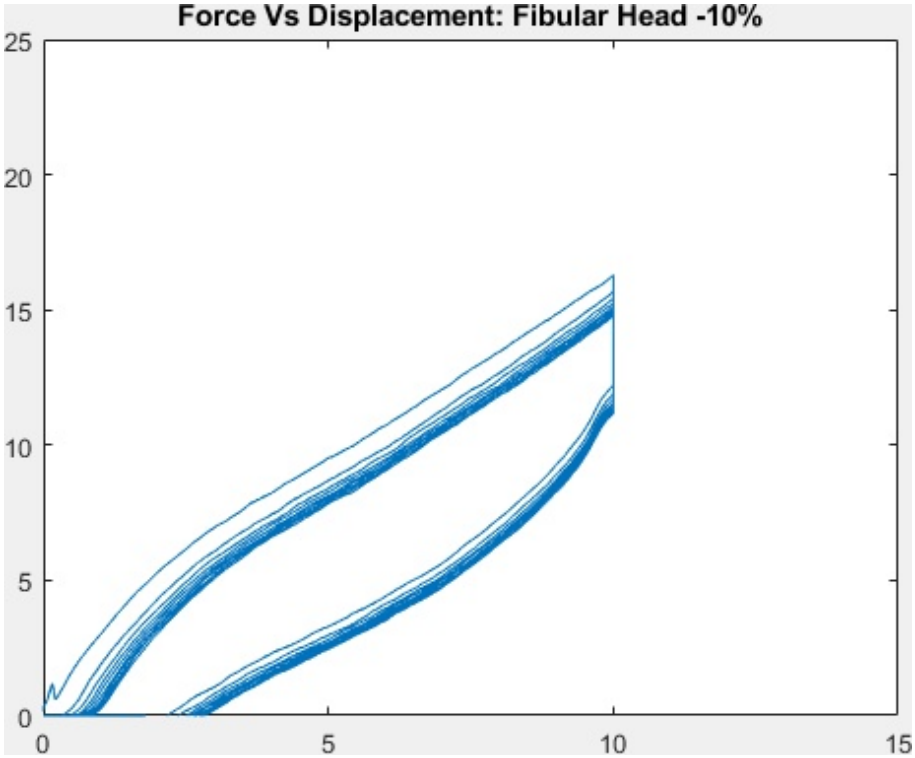

Figure 32: Pressure Vs Displacement 10 load cycles fibhead -10%

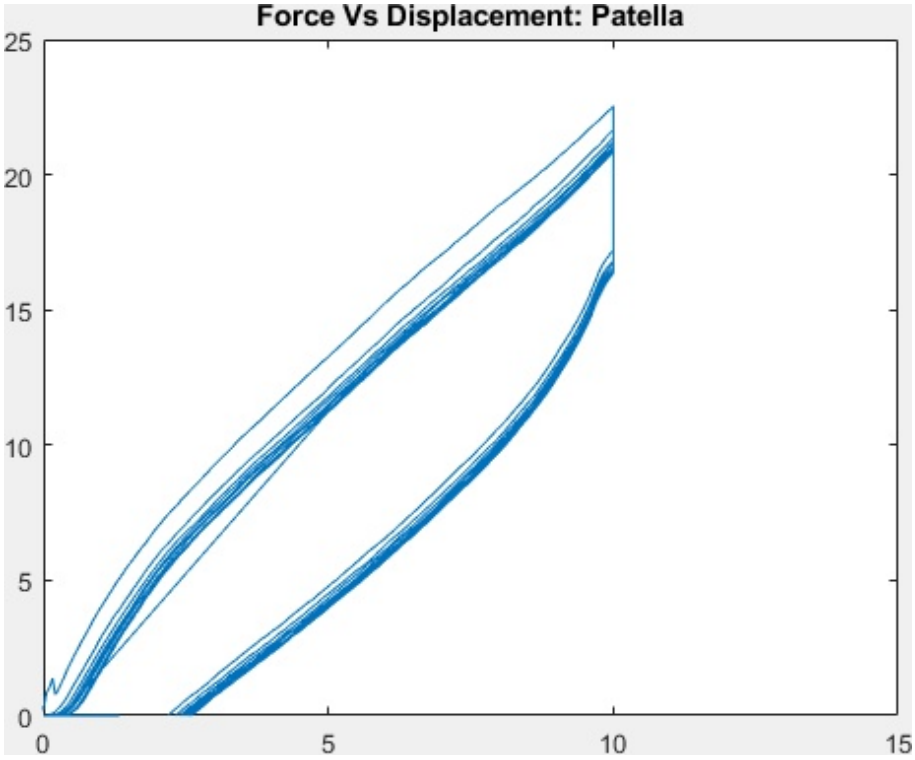

Figure 33: Pressure Vs Displacement 10 load cycles patella

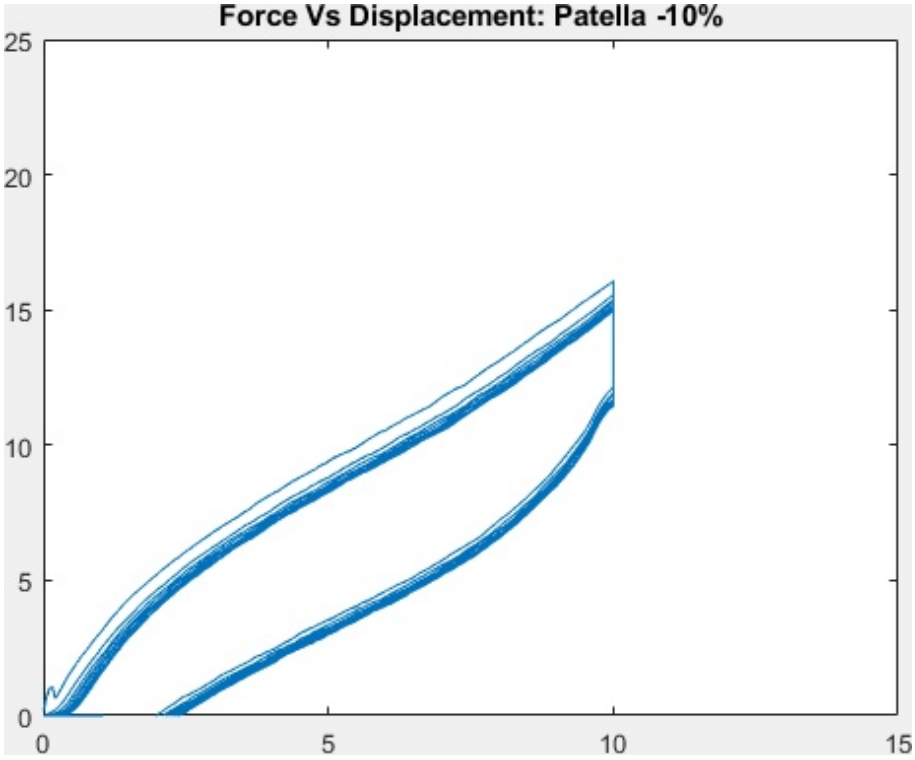

Figure 34: Pressure Vs Displacement 10 load cycles patella -10%

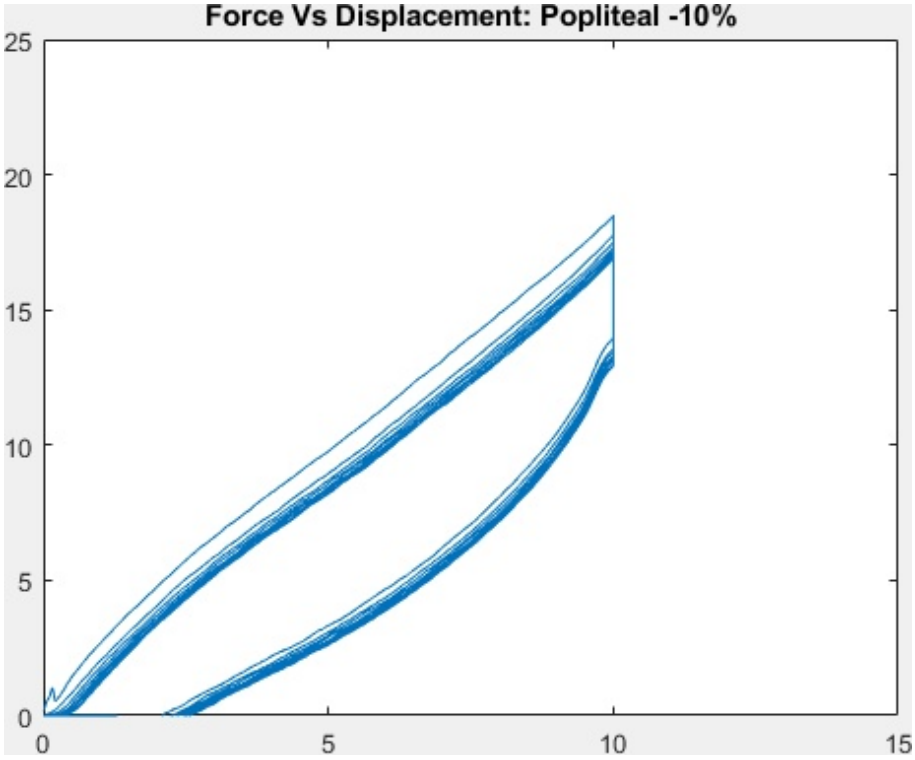

Figure 35: Pressure Vs Displacement 10 load cycles popliteal -10%

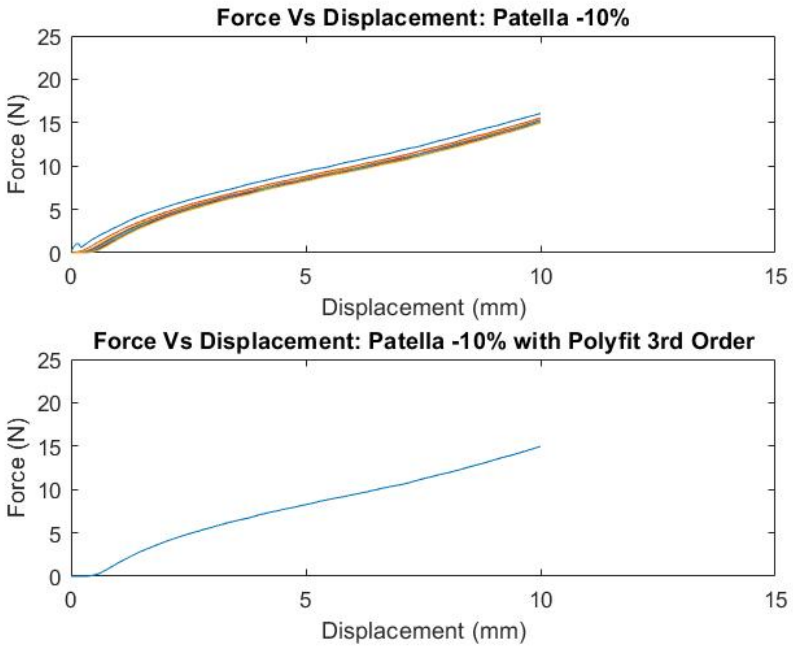

Figure 36: Pressure Vs Displacement 10 load cycles patella -10% polyfit

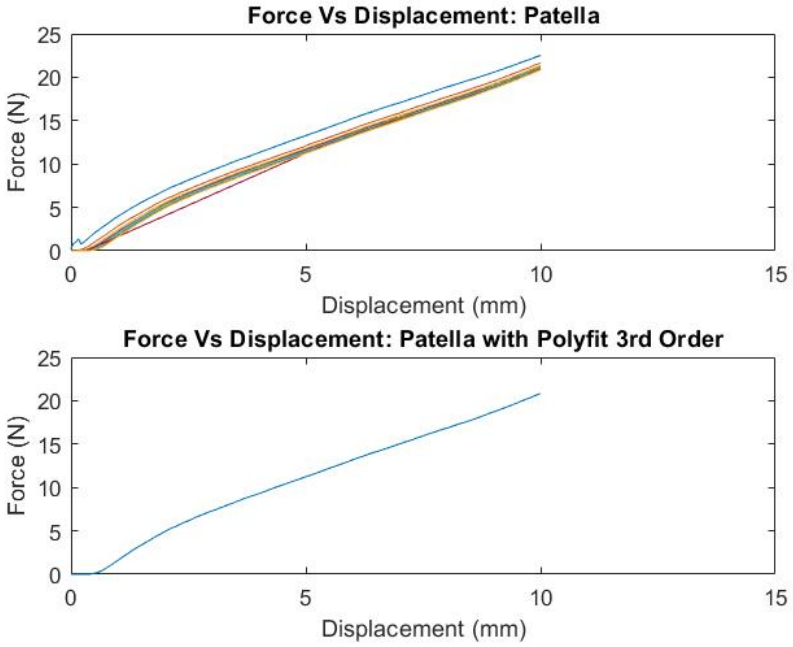

Figure 37: Pressure Vs Displacement 10 load cycles patella polyfit

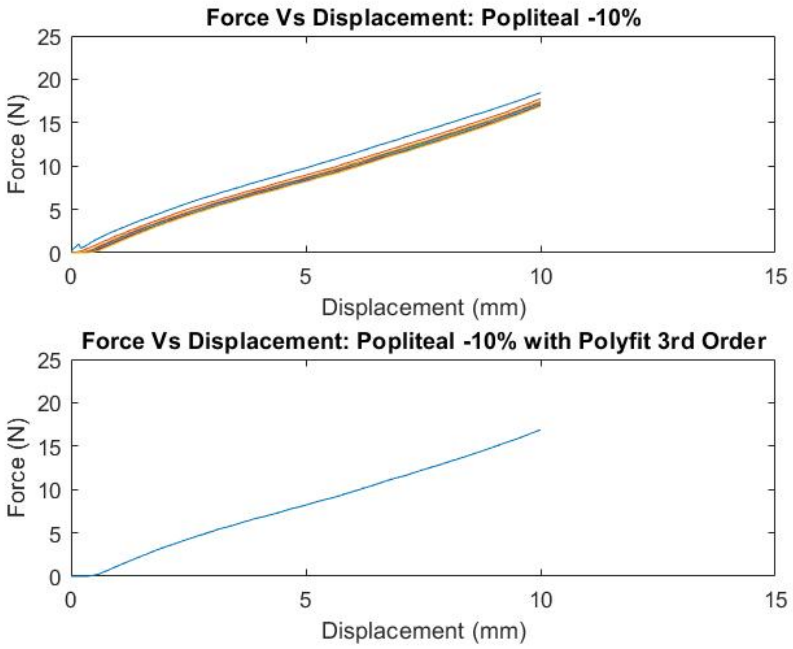

Figure 38: Pressure Vs Displacement 10 load cycles popliteal -10% polyfit

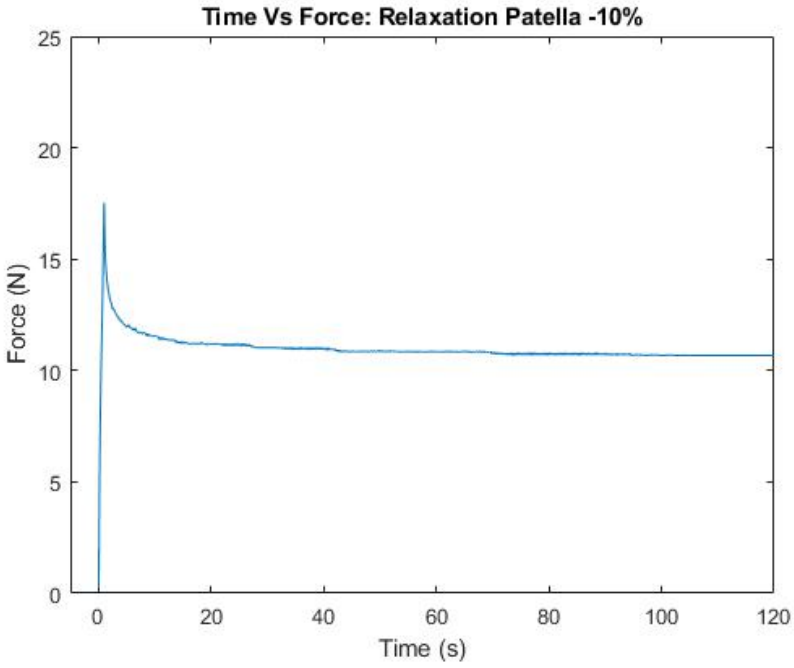

Figure 39: Force Vs Time Relaxation Curve Patella -10%

]

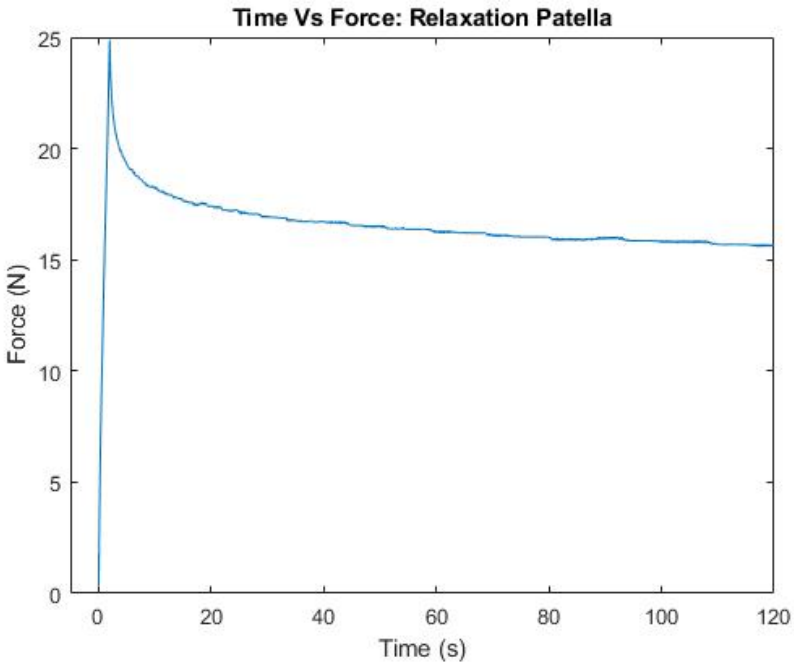

Figure 40: Force Vs Time Relaxation Curve Patella